Chapter 5

Equations with One Space Variable in Polar Coordinates

You're either part of the solution or you're part of the problem.

Eldridge Cleaver

5.1 Domain $0 \leq r < \infty$

5.1.1 Statement of the problem

$$\frac{\partial^\alpha T}{\partial t^\alpha} = a\left(\frac{\partial^2 T}{\partial r^2} + \frac{1}{r}\,\frac{\partial T}{\partial r}\right) + \Phi(r,t), \tag{5.1}$$

$$t = 0: \quad T = f(r), \qquad 0 < \alpha \leq 2, \tag{5.2}$$

$$t = 0: \quad \frac{\partial T}{\partial t} = F(r), \quad 1 < \alpha \leq 2, \tag{5.3}$$

$$\lim_{r\to\infty} T(r,t) = 0. \tag{5.4}$$

The solution:

$$T(r,t) = \int_0^\infty f(\rho)\,\mathcal{G}_f(r,\rho,t)\,\rho\,\mathrm{d}\rho + \int_0^\infty F(\rho)\,\mathcal{G}_F(r,\rho,t)\,\rho\,\mathrm{d}\rho + \int_0^t \int_0^\infty \Phi(\rho,\tau)\,\mathcal{G}_\Phi(r,\rho,t-\tau)\,\rho\,\mathrm{d}\rho\,\mathrm{d}\tau. \tag{5.5}$$

Y. Povstenko, *Linear Fractional Diffusion-Wave Equation for Scientists and Engineers*,
DOI 10.1007/978-3-319-17954-4_5

The fundamental solutions to the first Cauchy problem $\mathcal{G}_f(r,\rho,t)$, to the second Cauchy problem $\mathcal{G}_F(r,\rho,t)$ and to the source problem $\mathcal{G}_\Phi(r,\rho,t)$ were obtained in [148].

5.1.2 Fundamental solution to the first Cauchy problem

$$\frac{\partial^\alpha \mathcal{G}_f}{\partial t^\alpha} = a\left(\frac{\partial^2 \mathcal{G}_f}{\partial r^2} + \frac{1}{r}\frac{\partial \mathcal{G}_f}{\partial r}\right), \tag{5.6}$$

$$t=0: \quad \mathcal{G}_f = p_0\,\frac{\delta(r-\rho)}{r}, \qquad 0<\alpha\le 2, \tag{5.7}$$

$$t=0: \quad \frac{\partial \mathcal{G}_f}{\partial t} = 0, \qquad 1<\alpha\le 2. \tag{5.8}$$

It should be noted that the two-dimensional Dirac delta function in Cartesian coordinates $\delta(x)\,\delta(y)$ after passing to polar coordinates takes the form $\frac{1}{2\pi r}\,\delta(r)$, but for the sake of simplicity we have omitted the factor 2π in the solution (5.5) as well as the factor $\frac{1}{2\pi}$ in the delta term in (5.7). The condition at infinity (5.4) will be implied in all the problems in infinite domains considered in this chapter.

The Laplace transform with respect to time t and the Hankel transform of order 0 with respect to the radial variable r (2.78) give

$$\widehat{\mathcal{G}}_f^* = p_0 J_0(\rho\xi)\,\frac{s^{\alpha-1}}{s^\alpha + a\xi^2}. \tag{5.9}$$

The inverse integral transforms result in

$$\mathcal{G}_f(r,\rho,t) = p_0 \int\limits_0^\infty E_\alpha\left(-a\xi^2 t^\alpha\right) J_0(r\xi)\,J_0(\rho\xi)\,\xi\,d\xi. \tag{5.10}$$

It is convenient to introduce the following nondimensional quantities:

$$\bar r = \frac{r}{\rho}, \quad \eta = \rho\xi, \quad \kappa = \frac{\sqrt{a}\,t^{\alpha/2}}{\rho}, \quad \bar{\mathcal{G}}_f = \frac{\rho^2}{p_0}\,\mathcal{G}_f. \tag{5.11}$$

In this case

$$\bar{\mathcal{G}}_f = \int\limits_0^\infty E_\alpha\left(-\kappa^2\eta^2\right) J_0(\eta)\,J_0(\bar r\eta)\,\eta\,\mathrm{d}\eta. \tag{5.12}$$

Consider several particular cases of the solution (5.12).

Helmholtz equation ($\alpha \to 0$)

$$\bar{\mathcal{G}}_f = \begin{cases} \dfrac{1}{\kappa^2}\,I_0\left(\dfrac{\bar r}{\kappa}\right) K_0\left(\dfrac{1}{\kappa}\right), & 0\le \bar r<1,\\[2ex] \dfrac{1}{\kappa^2}\,I_0\left(\dfrac{1}{\kappa}\right) K_0\left(\dfrac{\bar r}{\kappa}\right), & 1<\bar r<\infty, \end{cases} \tag{5.13}$$

where $I_0(x)$ and $K_0(x)$ are the modified Bessel functions.

Subdiffusion with $\alpha = 1/2$

$$\bar{\mathcal{G}}_f = \frac{1}{2\sqrt{\pi}\kappa^2} \int_0^\infty \exp\left(-u^2 - \frac{1+\bar{r}^2}{8\kappa^2 u}\right) I_0\left(\frac{\bar{r}}{4\kappa^2 u}\right) \frac{1}{u}\, du. \tag{5.14}$$

Classical diffusion equation ($\alpha = 1$)

$$\bar{\mathcal{G}}_f = \frac{1}{2\kappa^2} \exp\left(-\frac{1+\bar{r}^2}{4\kappa^2}\right) I_0\left(\frac{\bar{r}}{2\kappa^2}\right). \tag{5.15}$$

Wave equation ($\alpha = 2$)

a) $0 < \kappa < 1$

$$\bar{\mathcal{G}}_f = \frac{1}{2\sqrt{1-\kappa}}\, \delta(\bar{r} - 1 + \kappa) + \frac{1}{2\sqrt{1+\kappa}}\, \delta(\bar{r} - 1 - \kappa)$$
$$+ \begin{cases} 0, & 0 \le \bar{r} < 1 - \kappa, \\ \dfrac{\kappa}{4\pi k^2 k'^2 \bar{r}^{3/2}} \left[\mathbf{E}(k) - k'^2 \mathbf{K}(k)\right], & 1 - \kappa < \bar{r} < 1 + \kappa, \\ 0, & 1 + \kappa < \bar{r} < \infty. \end{cases} \tag{5.16}$$

b) $\kappa > 1$

$$\bar{\mathcal{G}}_f = \frac{1}{2\sqrt{1+\kappa}}\, \delta(\bar{r} - 1 - \kappa)$$
$$+ \begin{cases} \dfrac{\kappa}{4\pi k k'^2 \bar{r}^{3/2}}\, \mathbf{E}\left(\dfrac{1}{k}\right), & 0 \le \bar{r} < \kappa - 1, \\ \dfrac{\kappa}{4\pi k^2 k'^2 \bar{r}^{3/2}} \left[\mathbf{E}(k) - k'^2 \mathbf{K}(k)\right], & \kappa - 1 < \bar{r} < 1 + \kappa, \\ 0, & 1 + \kappa < \bar{r} < \infty, \end{cases} \tag{5.17}$$

where $\mathbf{K}(k)$ and $\mathbf{E}(k)$ are the complete elliptic integrals of the first and second kind, respectively,

$$k = \frac{\sqrt{\kappa^2 - (\bar{r} - 1)^2}}{2\sqrt{\bar{r}}}, \qquad k' = \sqrt{1 - k^2}. \tag{5.18}$$

Dependence of the fundamental solution $\bar{\mathcal{G}}_f$ on nondimensional distance $\bar{r}$ is shown in Figs. 5.1 and 5.2 for various values of κ and α. In what follows, three distinguishing values of the parameter κ are considered: $0 < \kappa < 1$, $\kappa = 1$ and $\kappa > 1$. For a wave equation these values correspond to three characteristic events: the wave front does not yet arrive at the origin, the wave front arrives at the origin, and the wave front reflects from the origin.

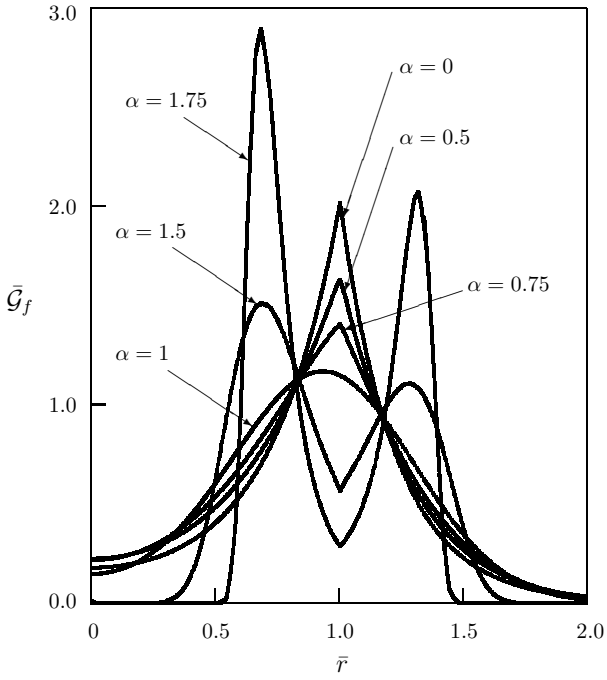

Figure 5.1: Dependence of the fundamental solution to the first Cauchy problem in a plane on distance; $\kappa = 0.25$ [148]

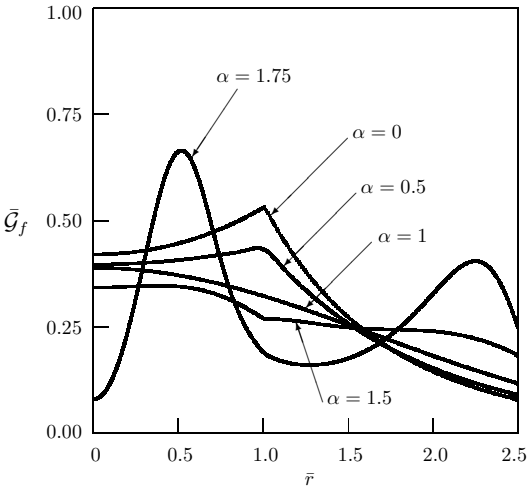

Figure 5.2: Dependence of the fundamental solution to the first Cauchy problem in a plane on distance; $\kappa = 1$

5.1.3 Fundamental solution to the second Cauchy problem

$$\frac{\partial^\alpha \mathcal{G}_F}{\partial t^\alpha} = a\left(\frac{\partial^2 \mathcal{G}_F}{\partial r^2} + \frac{1}{r}\frac{\partial \mathcal{G}_F}{\partial r}\right), \tag{5.19}$$

$$t = 0: \quad \mathcal{G}_F = 0, \qquad 1 < \alpha \le 2, \tag{5.20}$$

$$t = 0: \quad \frac{\partial \mathcal{G}_F}{\partial t} = w_0 \frac{\delta(r-\rho)}{r}, \qquad 1 < \alpha \le 2. \tag{5.21}$$

The solution:

$$\mathcal{G}_F(r,\rho,t) = w_0 t \int_0^\infty E_{\alpha,2}\left(-a\xi^2 t^\alpha\right) J_0(r\xi)\, J_0(\rho\xi)\, \xi\, d\xi. \tag{5.22}$$

Wave equation ($\alpha = 2$)

a) $0 < \kappa < 1$

$$\bar{\mathcal{G}}_F = \begin{cases} 0, & 0 \le \bar{r} < 1-\kappa, \\ \dfrac{1}{\kappa\pi\sqrt{\bar{r}}}\,\mathbf{K}(k), & 1-\kappa < \bar{r} < 1+\kappa, \\ 0, & 1+\kappa < \bar{r} < \infty. \end{cases} \tag{5.23}$$

b) $\kappa = 1$

$$\bar{\mathcal{G}}_F = \begin{cases} \dfrac{1}{\pi\sqrt{\bar{r}}}\,\mathbf{K}(k), & 0 < \bar{r} < 2, \\ 0, & 2 < \bar{r} < \infty. \end{cases} \tag{5.24}$$

c) $\kappa > 1$

$$\bar{\mathcal{G}}_F = \begin{cases} \dfrac{1}{\kappa\pi k\sqrt{\bar{r}}}\,\mathbf{K}\left(\dfrac{1}{k}\right), & 0 \le \bar{r} < \kappa - 1, \\ \dfrac{1}{\kappa\pi\sqrt{\bar{r}}}\,\mathbf{K}(k), & \kappa - 1 < \bar{r} < 1+\kappa, \\ 0, & 1+\kappa < \bar{r} < \infty, \end{cases} \tag{5.25}$$

where $\bar{\mathcal{G}}_F = \rho^2 \mathcal{G}_F/(w_0 t)$, other nondimensional quantities are the same as in (5.11).

Dependence of the fundamental solution to the second Cauchy problem on distance is shown in Figs. 5.3–5.5.

In the case of the wave equation ($\alpha = 2$) the fundamental solution has jumps at $\bar{r} = 1-\kappa$ and at $\bar{r} = 1+\kappa$ for $0 < \kappa < 1$, has a singularity at the origin $\bar{r} = 0$ for $\kappa = 1$, and has a singularity at $\bar{r} = \kappa - 1$ and a jump at $\bar{r} = \kappa + 1$ for $\kappa > 1$.

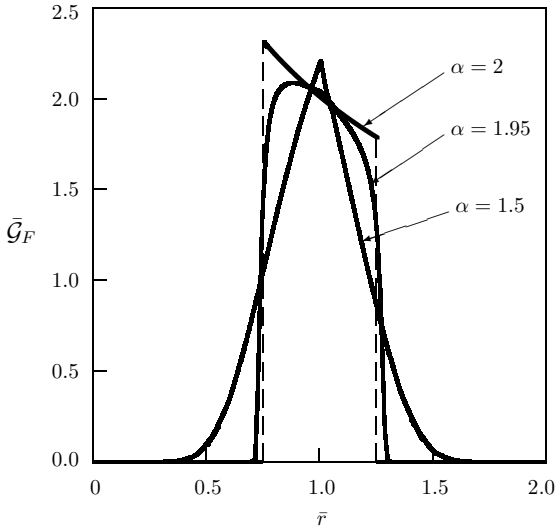

Figure 5.3: Dependence of the fundamental solution to the second Cauchy problem in a plane on distance; $\kappa = 0.25$ [148]

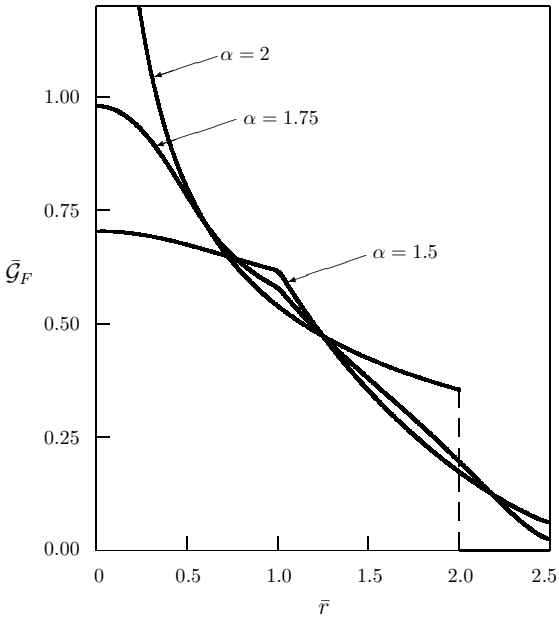

Figure 5.4: Dependence of the fundamental solution to the second Cauchy problem in a plane on distance; $\kappa = 1$

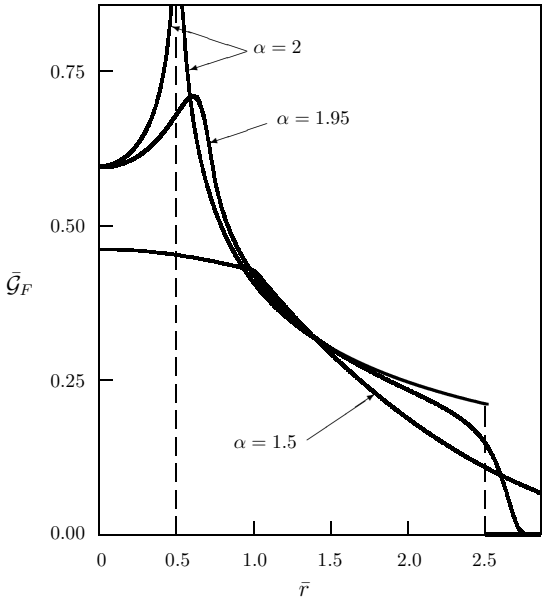

Figure 5.5: Dependence of the fundamental solution to the second Cauchy problem in a plane on distance; $\kappa = 1.5$ [148]

5.1.4 Fundamental solution to the source problem

The fundamental solution to the source problem is obtained in the similar way and has the following form:

$$\mathcal{G}_\Phi(r,\rho,t) = q_0 t^{\alpha-1} \int_0^\infty E_{\alpha,\alpha}\left(-a\xi^2 t^\alpha\right) J_0(r\xi)\, J_0(\rho\xi)\, \xi\, d\xi. \tag{5.26}$$

Dependence of the fundamental solution $\bar{\mathcal{G}}_\Phi = \rho^2 \mathcal{G}_\Phi / (q_0 t^{\alpha-1})$ on distance is shown in Figs. 5.6–5.8.

5.1.5 Delta-pulse at the origin

In the case of the first Cauchy problem we have

$$\frac{\partial^\alpha T}{\partial t^\alpha} = a\left(\frac{\partial^2 T}{\partial r^2} + \frac{1}{r}\frac{\partial T}{\partial r}\right), \tag{5.27}$$

$$t = 0: \quad T = p_0 \frac{\delta(r)}{2\pi r}, \qquad 0 < \alpha \le 2, \tag{5.28}$$

$$t = 0: \quad \frac{\partial T}{\partial t} = 0, \qquad 1 < \alpha \le 2\,. \tag{5.29}$$

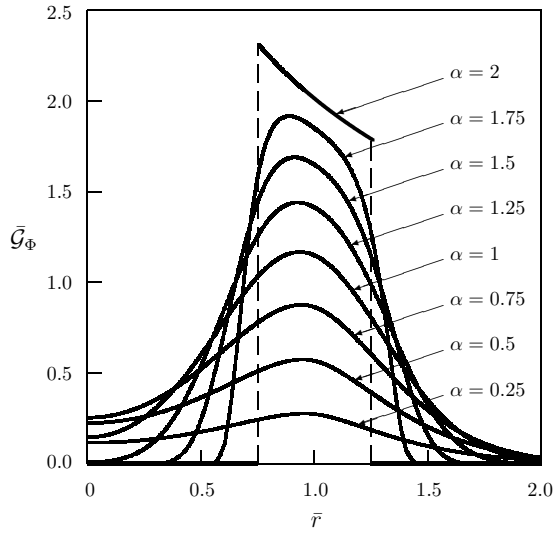

Figure 5.6: Dependence of the fundamental solution to the source problem in a plane on distance; $\kappa = 0.25$ [148]

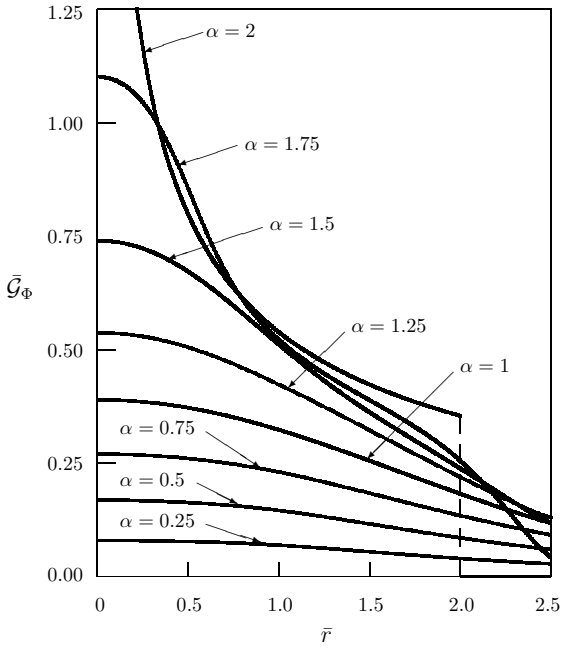

Figure 5.7: Dependence of the fundamental solution to the source problem in a plane on distance; $\kappa = 1$ [148]

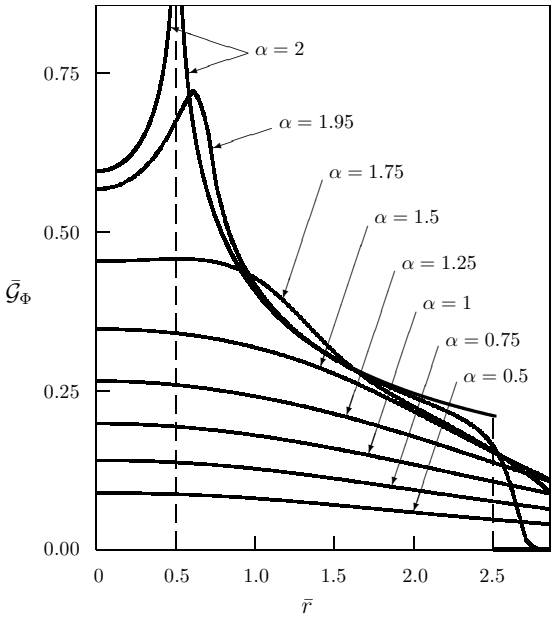

Figure 5.8: Dependence of the fundamental solution to the source problem in a plane on distance; $\kappa = 1.5$ [148]

The solution:

$$T = \frac{p_0}{2\pi} \int_0^\infty E_\alpha \left(-a\xi^2 t^\alpha\right) J_0(r\xi)\, \xi \, d\xi \tag{5.30}$$

and

$$\overline{T} = \frac{1}{2\pi} \int_0^\infty E_\alpha \left(-\eta^2\right) J_0(\bar{r}\eta)\, \eta \, \mathrm{d}\eta, \tag{5.31}$$

where

$$\bar{r} = \frac{r}{\sqrt{a} t^{\alpha/2}}, \quad \eta = \sqrt{a} t^{\alpha/2} \xi, \quad \overline{T} = \frac{a t^\alpha}{p_0} T. \tag{5.32}$$

Helmholtz equation ($\alpha \to 0$)

$$\overline{T} = \frac{1}{2\pi} K_0(\bar{r}). \tag{5.33}$$

Here $K_0(r)$ is the modified Bessel function.

Subdiffusion with $\alpha = 1/2$

$$\overline{T} = \frac{1}{4\pi^{3/2}} \int_0^\infty \frac{1}{u} \exp\left(-u^2 - \frac{\bar{r}^2}{8u}\right) du. \tag{5.34}$$

Classical diffusion equation ($\alpha = 1$)

$$\overline{T} = \frac{1}{4\pi} \exp\left(-\frac{\bar{r}^2}{4}\right). \tag{5.35}$$

Wave equation ($\alpha = 2$)

$$T = \frac{p_0}{2\pi\sqrt{a}} \frac{\partial}{\partial t} \frac{H(\sqrt{a}t - r)}{\sqrt{at^2 - r^2}}, \tag{5.36}$$

where $H(x)$ is the Heaviside step function (see also [85]).

Now we investigate the behavior of the solution (5.31) at the origin. As for large values of η we have (see (2.161)):

$$E_\alpha(-\eta^2) \sim \frac{1}{\Gamma(1-\alpha)\,\eta^2} \qquad \text{for } \eta \to \infty, \quad 0 < \alpha < 2, \tag{5.37}$$

only the fundamental solution to the classical diffusion equation has no singularity at the origin. To investigate the type of singularity we rewrite the solution (5.31) in the following form:

$$\begin{aligned} \overline{T} = {} & \frac{1}{2\pi} \int_0^\infty \left[E_\alpha(-\eta^2) - \frac{1}{\Gamma(1-\alpha)(1+\eta^2)} \right] J_0(\bar{r}\eta)\,\eta\,d\eta \\ & + \frac{1}{2\pi\Gamma(1-\alpha)} \int_0^\infty \frac{1}{1+\eta^2} J_0(\bar{r}\eta)\,\eta\,d\eta. \end{aligned} \tag{5.38}$$

The first integral in (5.38) has no singularity at the origin, while the second one can be calculated analytically (see equation (A.28) from the Appendix) and yields the logarithmic singularity at the origin

$$\overline{T} \sim \frac{1}{2\pi\Gamma(1-\alpha)} K_0(\bar{r}), \qquad 0 < \alpha < 2, \tag{5.39}$$

or

$$\overline{T} \sim -\frac{1}{2\pi\Gamma(1-\alpha)} \ln \bar{r}, \qquad 0 < \alpha < 2. \tag{5.40}$$

Comparison of (5.40) and (5.33) allows us to substitute the condition $0 < \alpha < 2$ by $0 \le \alpha < 2$. Equation (5.40), rewritten in terms of dimensional solution T,

$$T \sim -\frac{p_0}{2\pi a t^\alpha \Gamma(1-\alpha)} \ln \bar{r}, \qquad 0 \le \alpha < 2, \tag{5.41}$$

is consistent with the behavior of the solution for small values of r obtained in [208].

Dependence of the nondimensional solution $\overline{T}$ on the similarity variable $\bar{r}$ is shown in Fig. 5.9.

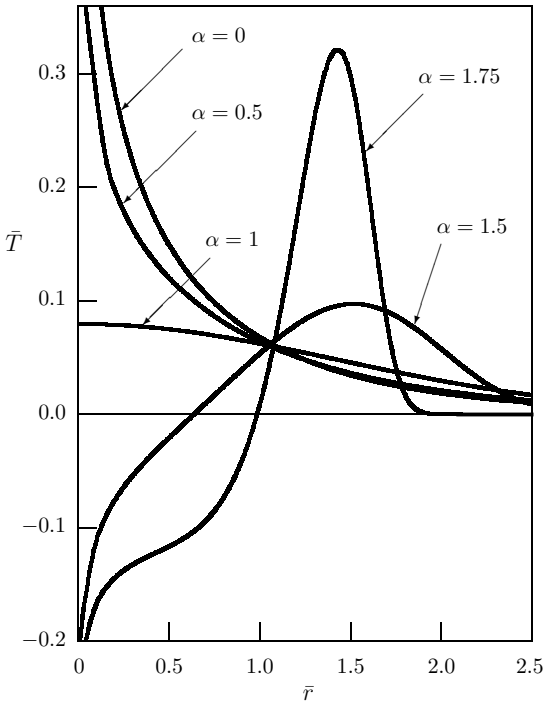

Figure 5.9: Dependence of the solution on the similarity variable $\bar{r}$ (the first Cauchy problem in a plane with the delta-pulse initial condition)

In the case of the second Cauchy problem with the delta-pulse initial condition the solution is expressed as

$$T = \frac{w_0 t}{2\pi} \int_0^\infty E_{\alpha,2}(-a\xi^2 t^\alpha)\, J_0(r\xi)\, \xi \, d\xi \tag{5.42}$$

with $\overline{T} = at^{\alpha-1}T/w_0$.

The particular case of the solution (5.42) for the wave equation ($\alpha = 2$) reads

$$\overline{T} = \begin{cases} \dfrac{1}{2\pi\sqrt{1-\bar{r}^2}}, & 0 < \bar{r} < 1, \\ 0, & 1 < \bar{r} < \infty. \end{cases} \tag{5.43}$$

To investigate behavior of the solution (5.42) at the origin we recall that for large values of η we have (see (2.162)):

$$E_{\alpha,2}(-\eta^2) \sim \frac{1}{\Gamma(2-\alpha)\,\eta^2} \quad \text{for } \eta \to \infty, \quad 1 < \alpha < 2. \tag{5.44}$$

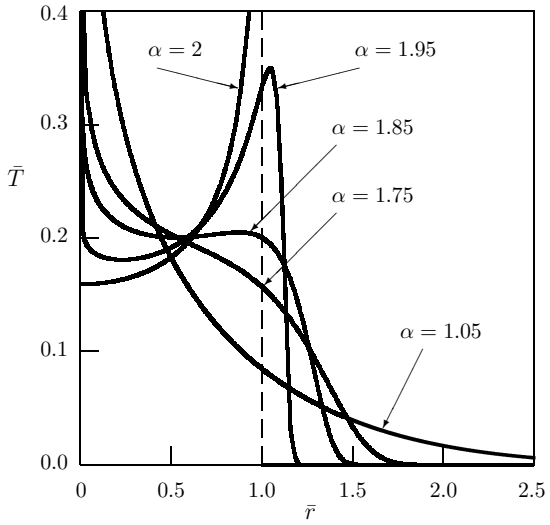

Figure 5.10: Dependence of the solution on the similarity variable $\bar{r}$ (the second Cauchy problem in a plane with the delta-pulse initial condition)

Computations similar to those carried out above lead to

$$\overline{T} \sim -\frac{1}{2\pi\Gamma(2-\alpha)} \ln \bar{r}, \qquad 1 < \alpha < 2. \tag{5.45}$$

Hence, in the case of the second Cauchy problem with the delta-pulse initial condition the solution also has its logarithmic singularity at the origin.

Dependence of nondimensional solution $\overline{T}$ on the similarity variable is depicted in Fig. 5.10.

The solution to the time-fractional diffusion wave equation with the source term $q_0 \frac{\delta(r)}{2\pi r}\, \delta(t)$ under zero initial conditions is expressed as

$$T = \frac{q_0 t^{\alpha-1}}{2\pi} \int\limits_0^\infty E_{\alpha,\alpha}\left(-a\xi^2 t^\alpha\right) J_0(r\xi)\, \xi\, d\xi. \tag{5.46}$$

It should be noted that due to (2.163)

$$E_{\alpha,\alpha}(-\eta^2) \sim -\frac{1}{\Gamma(-\alpha)\,\eta^4} \quad \text{for } \eta \to \infty, \quad 0 < \alpha < 2. \tag{5.47}$$

Hence, the solution (5.46) has no singularity at the origin for all $0 < \alpha < 2$.

Dependence of nondimensional solution $\overline{T} = atT/q_0$ on the similarity variable is depicted in Fig. 5.11. It should be emphasized that solution (5.43), the same

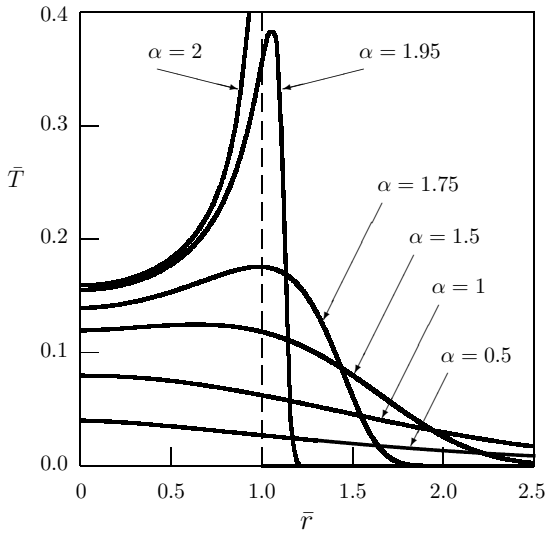

Figure 5.11: Dependence of the solution on the similarity variable $\bar{r}$ (the delta pulse source problem in a plane with zero initial conditions)

both for the source problem and the second Cauchy problem, is approximated by solutions (5.42) and (5.46) with $\alpha \to 2$ in different ways, in particular the solution (5.42) has the logarithmic singularity at the origin, whereas the solution (5.46) has no singularity.

5.2 Evolution of the unit-box signal

5.2.1 First Cauchy problem

$$\frac{\partial^\alpha T}{\partial t^\alpha} = a\left(\frac{\partial^2 T}{\partial r^2} + \frac{1}{r}\frac{\partial T}{\partial r}\right), \tag{5.48}$$

$$t = 0: \quad T = \begin{cases} T_0, & 0 \le r < R, \\ 0, & R < r < \infty, \end{cases} \qquad 0 < \alpha \le 2, \tag{5.49}$$

$$t = 0: \quad \frac{\partial T}{\partial t} = 0, \qquad 1 < \alpha \le 2. \tag{5.50}$$

The solution [162]:

$$T = T_0 R \int_0^\infty E_\alpha\left(-a\xi^2 t^\alpha\right) J_1(R\xi)\, J_0(r\xi)\, d\xi. \tag{5.51}$$

It is convenient to introduce the following nondimensional quantities:

$$\bar{r} = \frac{r}{R}, \qquad \kappa = \frac{\sqrt{a}t^{\alpha/2}}{R}, \qquad \overline{T} = \frac{T}{T_0}. \tag{5.52}$$

Helmholtz equation ($\alpha \to 0$)

$$\overline{T} = \begin{cases} \dfrac{1}{\kappa}\left[\bar{r} I_1\left(\dfrac{\bar{r}}{\kappa}\right) K_0\left(\dfrac{\bar{r}}{\kappa}\right) + \bar{r} I_0\left(\dfrac{\bar{r}}{\kappa}\right) K_1\left(\dfrac{\bar{r}}{\kappa}\right) - I_0\left(\dfrac{\bar{r}}{\kappa}\right) K_1\left(\dfrac{1}{\kappa}\right)\right], & \\ & 0 \le \bar{r} < 1, \\ \dfrac{1}{\kappa} I_1\left(\dfrac{1}{\kappa}\right) K_0\left(\dfrac{\bar{r}}{\kappa}\right), & 1 < \bar{r} < \infty. \end{cases} \tag{5.53}$$

Subdiffusion with $\alpha = 1/2$

$$\overline{T} = \frac{1}{4\kappa^2\sqrt{\pi}} \int_0^\infty \frac{1}{u} \mathrm{e}^{-u^2} \int_0^1 \exp\left(-\frac{\bar{r}^2 + x}{8\kappa^2 u}\right) I_0\left(\frac{\bar{r}\sqrt{x}}{4\kappa^2 u}\right) \mathrm{d}x \, \mathrm{d}u. \tag{5.54}$$

Classical diffusion equation ($\alpha = 1$)

$$\overline{T} = \frac{1}{4\kappa^2} \int_0^1 \exp\left(-\frac{\bar{r}^2 + x}{4\kappa^2}\right) I_0\left(\frac{\bar{r}\sqrt{x}}{2\kappa^2}\right) dx. \tag{5.55}$$

Wave equation ($\alpha = 2$)

a) $0 < \kappa < 1$

$$\overline{T} = \begin{cases} 1, & 0 \le \bar{r} < 1 - \kappa, \\ 1 - \Lambda_0\left(\arcsin\sqrt{\dfrac{2\bar{r}}{1 + \bar{r} + \kappa}}, k\right) + \dfrac{\bar{r} - \kappa}{\pi\sqrt{\bar{r}}} \mathbf{K}(k), & 1 - \kappa < \bar{r} < 1 + \kappa, \\ 0, & 1 + \kappa < \bar{r} < \infty. \end{cases} \tag{5.56}$$

b) $\kappa = 1$

$$\overline{T} = \begin{cases} 1 - \Lambda_0\left(\arcsin\sqrt{\dfrac{2\bar{r}}{2 + \bar{r}}}, k\right) + \dfrac{\bar{r} - 1}{\pi\sqrt{\bar{r}}} \mathbf{K}(k), & 0 \le \bar{r} < 2, \\ 0, & 2 < \bar{r} < \infty. \end{cases} \tag{5.57}$$

c) $1 < \kappa < \infty$

$$\bar{T} = \begin{cases} 1 - \Lambda_0 \left(\arcsin \sqrt{\dfrac{\kappa + \bar{r} - 1}{\kappa + \bar{r} + 1}}, \dfrac{1}{k} \right) \\ \qquad - \dfrac{1}{\pi k \sqrt{\bar{r}}} \mathbf{K}\left(\dfrac{1}{k}\right), & 0 \le \bar{r} < \kappa - 1, \\ 1 - \Lambda_0 \left(\arcsin \sqrt{\dfrac{2\bar{r}}{\kappa + \bar{r} + 1}}, k \right) \\ \qquad + \dfrac{\bar{r} - \kappa}{\pi \sqrt{\bar{r}}} \mathbf{K}(k), & \kappa - 1 < \bar{r} < 1 + \kappa, \\ 0, & 1 + \kappa < \bar{r} < \infty. \end{cases} \tag{5.58}$$

where $\Lambda_0(\varphi, k)$ is the Heuman Lambda function,

$$\Lambda_0(\varphi, k) = \frac{2}{\pi} \left[\mathbf{E}(k) F(\varphi, k') + \mathbf{K}(k) E(\varphi, k') - \mathbf{K}(k) F(\varphi, k') \right], \tag{5.59}$$

$F(\varphi, k)$ and $E(\varphi, k)$ are elliptic integrals of the first and second kind, $\mathbf{K}(k)$ and $\mathbf{E}(k)$ are complete elliptic integrals of the first and second kind, respectively, k and k' are the same as in (5.18).

The solution (5.51) is shown in Figs. 5.12–5.14.

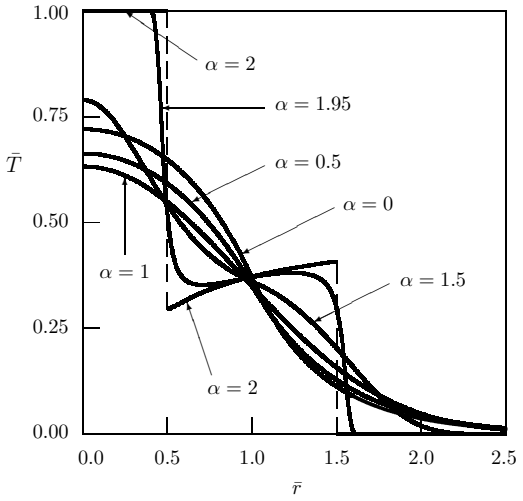

Figure 5.12: Evolution of the unit-box signal in a plane (the first Cauchy problem; $\kappa = 0.5$) [162]

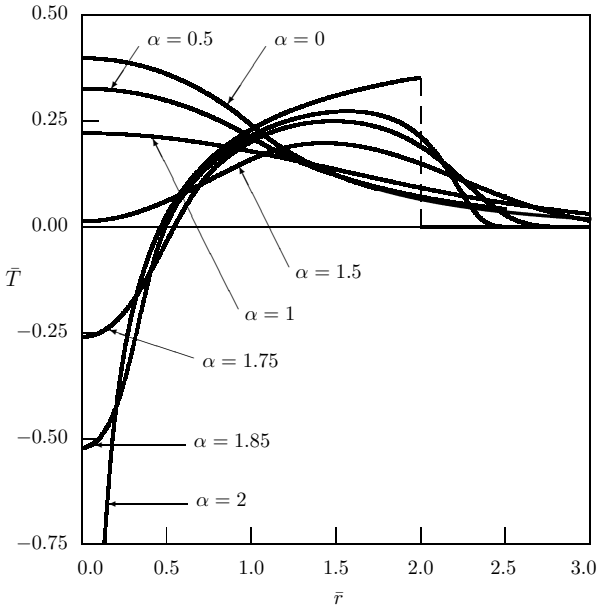

Figure 5.13: Evolution of the unit-box signal in a plane (the first Cauchy problem; $\kappa = 1$) [162]

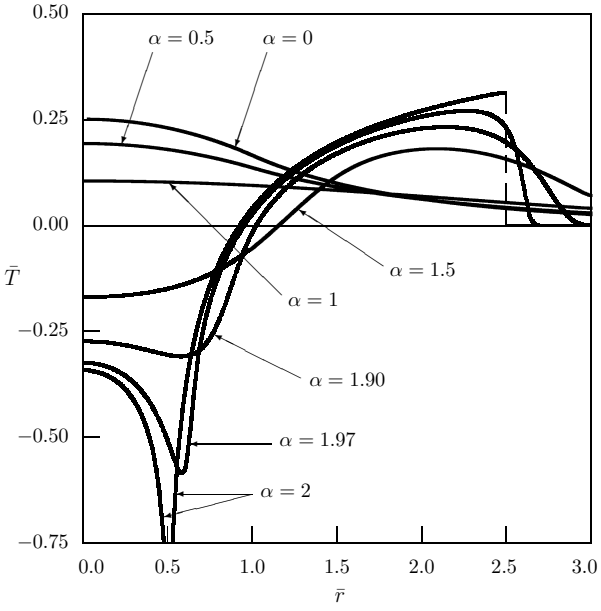

Figure 5.14: Evolution of the unit-box signal in a plane (the first Cauchy problem; $\kappa = 1.5$) [162]

5.2.2 Second Cauchy problem

$$\frac{\partial^\alpha T}{\partial t^\alpha} = a\left(\frac{\partial^2 T}{\partial r^2} + \frac{1}{r}\frac{\partial T}{\partial r}\right), \tag{5.60}$$

$$t = 0: \quad T = 0, \qquad 1 < \alpha \le 2, \tag{5.61}$$

$$t = 0: \quad \frac{\partial T}{\partial t} = \begin{cases} w_0, & 0 \le r < R, \\ 0, & R < r < \infty, \end{cases} \qquad 1 < \alpha \le 2. \tag{5.62}$$

The solution [182]:

$$T = w_0 R t \int_0^\infty E_{\alpha,2}\left(-a\xi^2 t^\alpha\right) J_1(R\xi)\, J_0(r\xi)\, \mathrm{d}\xi. \tag{5.63}$$

Dependence of solution (5.63) on distance is shown in Figs. 5.15–5.17 for various values of κ and α ($\overline{T} = T/(w_0 t)$, $\bar{r} = r/R$).

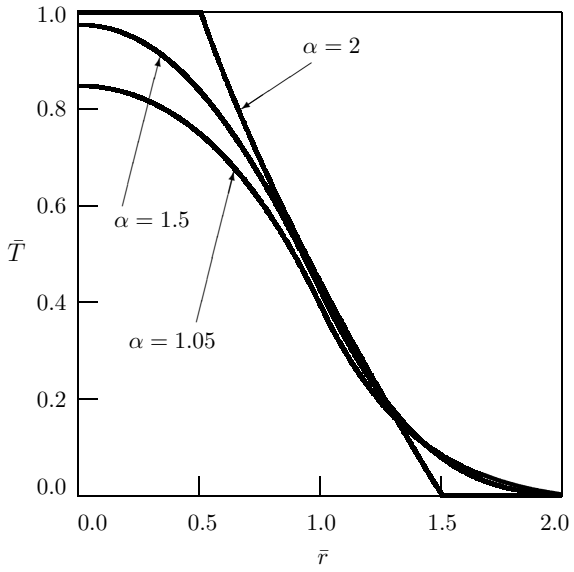

Figure 5.15: Evolution of the unit-box signal in a plane (the second Cauchy problem; $\kappa = 0.5$) [182]

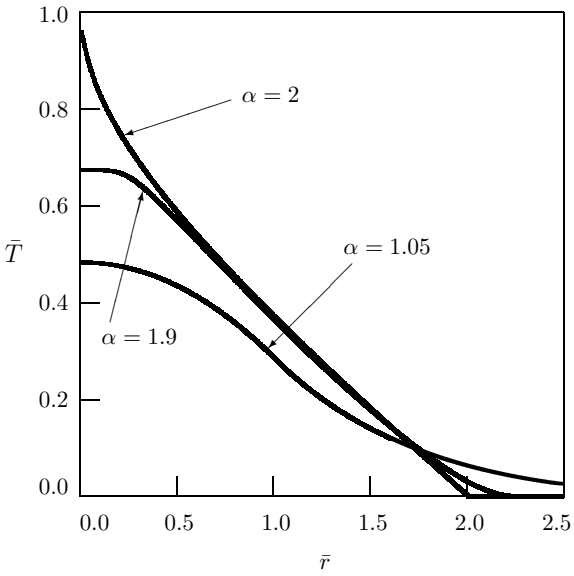

Figure 5.16: Evolution of the unit-box signal in a plane (the second Cauchy problem; $\kappa = 1$)

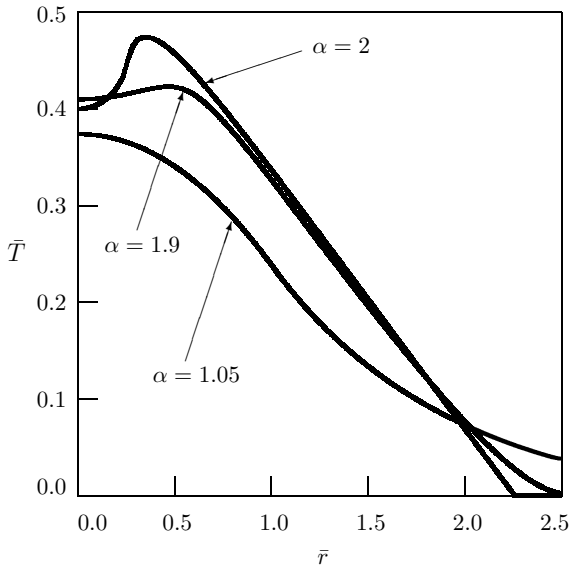

Figure 5.17: Evolution of the unit-box signal in a plane (the second Cauchy problem; $\kappa = 1.25$) [182]

5.2.3 Source problem

We consider the diffusion-wave equation

$$\frac{\partial^\alpha T}{\partial t^\alpha} = a\left(\frac{\partial^2 T}{\partial r^2} + \frac{1}{r}\frac{\partial T}{\partial r}\right) + \delta(t)\begin{cases} q_0, & 0 \le r < R, \\ 0, & R < r < \infty, \end{cases} \tag{5.64}$$

under zero initial conditions. The solution has the following form [182]:

$$T = q_0 R t^{\alpha-1} \int_0^\infty E_{\alpha,\alpha}(-a\xi^2 t^\alpha)\, J_0(r\xi)\, J_1(R\xi)\, \mathrm{d}\xi. \tag{5.65}$$

Figures 5.18–5.20 show the solution (5.65) for various values of α and κ ($\overline{T} = t^{1-\alpha}T/q_0$).

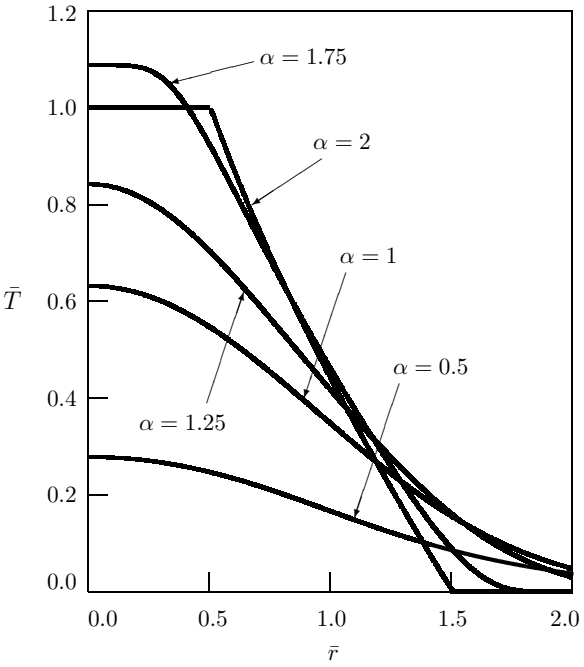

Figure 5.18: Evolution of the unit-box signal in a plane (the source problem; $\kappa = 0.5$) [182]

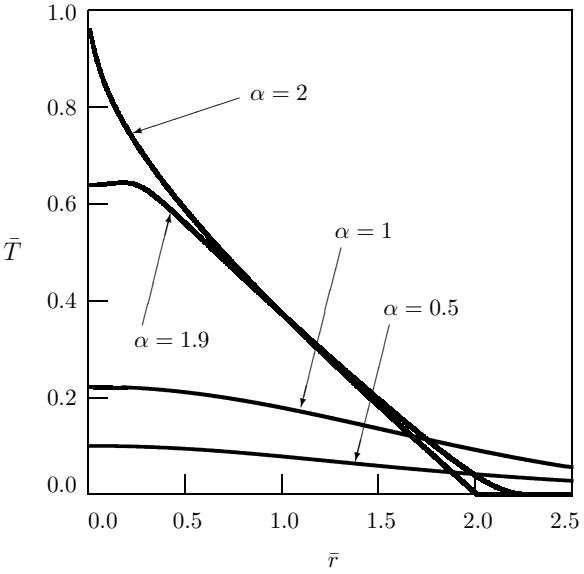

Figure 5.19: Evolution of the unit-box signal in a plane (the source problem; $\kappa = 1$)

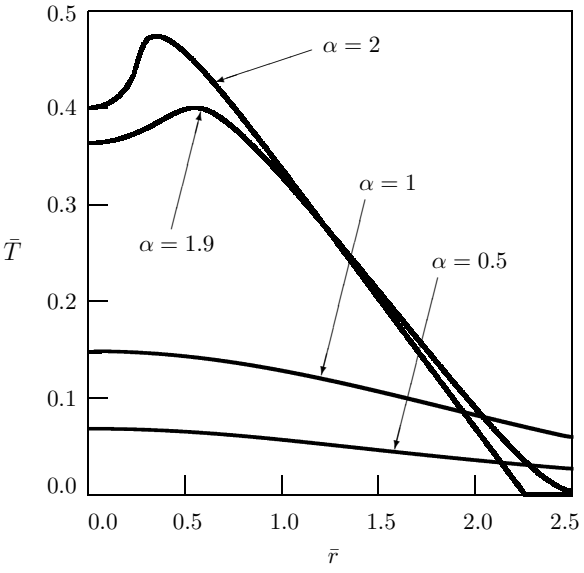

Figure 5.20: Evolution of the unit-box signal in a plane (the source problem; $\kappa = 1.25$) [182]

5.3 Domain $0 < r < R$

5.3.1 Dirichlet boundary condition

$$\frac{\partial^\alpha T}{\partial t^\alpha} = a\left(\frac{\partial^2 T}{\partial r^2} + \frac{1}{r}\,\frac{\partial T}{\partial r}\right) + \Phi(r,t), \tag{5.66}$$

$$t = 0: \quad T = f(r), \qquad 0 < \alpha \le 2, \tag{5.67}$$

$$t = 0: \quad \frac{\partial T}{\partial t} = F(r), \quad 1 < \alpha \le 2, \tag{5.68}$$

$$r = R: \quad T = g(t). \tag{5.69}$$

The solution:

$$T(r,t) = \int_0^R f(\rho)\,\mathcal{G}_f(r,\rho,t)\,\rho\,\mathrm{d}\rho + \int_0^R F(\rho)\,\mathcal{G}_F(r,\rho,t)\,\rho\,\mathrm{d}\rho$$
$$+ \int_0^t \int_0^R \Phi(\rho,\tau)\,\mathcal{G}_\Phi(r,\rho,t-\tau)\,\rho\,\mathrm{d}\rho\,\mathrm{d}\tau + \int_0^t g(\tau)\,\mathcal{G}_g(r,t-\tau)\,\mathrm{d}\tau. \tag{5.70}$$

The fundamental solutions under zero Dirichlet boundary condition have the form

$$\begin{pmatrix} \mathcal{G}_f(r,\rho,t) \\ \mathcal{G}_F(r,\rho,t) \\ \mathcal{G}_\Phi(r,\rho,t) \end{pmatrix} = \frac{2}{R^2}\sum_{k=1}^{\infty} \begin{pmatrix} p_0\,E_\alpha(-a\xi_k^2 t^\alpha) \\ w_0 t\,E_{\alpha,2}(-a\xi_k^2 t^\alpha) \\ q_0 t^{\alpha-1}\,E_{\alpha,\alpha}(-a\xi_k^2 t^\alpha) \end{pmatrix} \frac{J_0(r\xi_k)J_0(\rho\xi_k)}{J_1^2(R\xi_k)} \tag{5.71}$$

with the sum over all positive roots of the zero-order Bessel function

$$J_0(R\xi_k) = 0. \tag{5.72}$$

They are obtained using the Laplace transform with respect to time t and the finite Hankel transform (2.96) with respect to the radial coordinate r.

The fundamental solution to the Dirichlet problem under zero initial condition is expressed as

$$\mathcal{G}_g(r,t) = -\frac{aRg_0}{q_0}\,\frac{\partial \mathcal{G}_\Phi(r,\rho,t)}{\partial \rho}\bigg|_{\rho=R}. \tag{5.73}$$

For numerical calculations the following nondimensional quantities are introduced:

$$\bar{r} = \frac{r}{R}, \qquad \bar{\rho} = \frac{\rho}{R}, \qquad \kappa = \frac{\sqrt{a}t^{\alpha/2}}{R}, \qquad \overline{\mathcal{G}}_f = \frac{R^2}{p_0}\,\mathcal{G}_f,$$

$$\overline{\mathcal{G}}_F = \frac{R^2}{w_0 t}\,\mathcal{G}_F, \qquad \overline{\mathcal{G}}_\Phi = \frac{R^2}{q_0 t^{\alpha-1}}\,\mathcal{G}_\Phi, \qquad \overline{\mathcal{G}}_g = \frac{R^2}{a g_0 t^{\alpha-1}}\,\mathcal{G}_g. \tag{5.74}$$

Dependence of the fundamental solution $\overline{\mathcal{G}}_f$ on the nondimensional distance r is shown in Figs. 5.21–5.22. Dependence of the fundamental solution $\overline{\mathcal{G}}_F$ on distance is presented in Figs. 5.23–5.25. Dependence of the fundamental solution $\overline{\mathcal{G}}_\Phi$ on distance is depicted in Figs. 5.26–5.28. The fundamental solution to the Dirichlet problem $\overline{\mathcal{G}}_g$ is shown in Fig. 5.29.

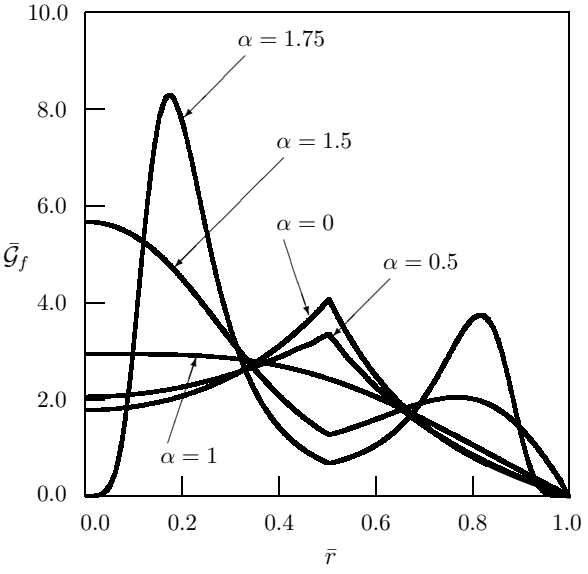

Figure 5.21: The fundamental solution to the first Cauchy problem in a cylinder under zero Dirichlet boundary condition ($\bar{\rho} = 0.5$, $\kappa = 0.25$)

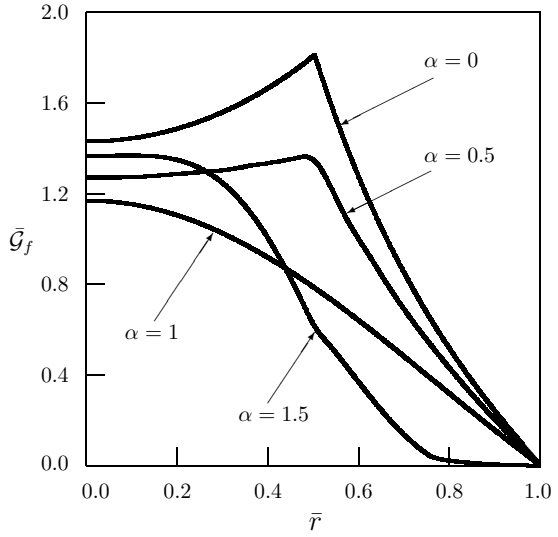

Figure 5.22: The fundamental solution to the first Cauchy problem in a cylinder under zero Dirichlet boundary condition ($\bar{\rho} = 0.5$, $\kappa = 0.5$)

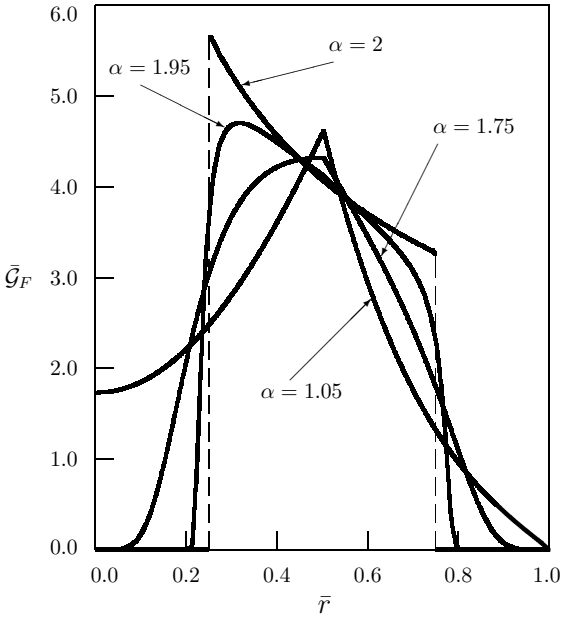

Figure 5.23: The fundamental solution to the second Cauchy problem in a cylinder under zero Dirichlet boundary condition ($\bar{\rho} = 0.5$, $\kappa = 0.25$)

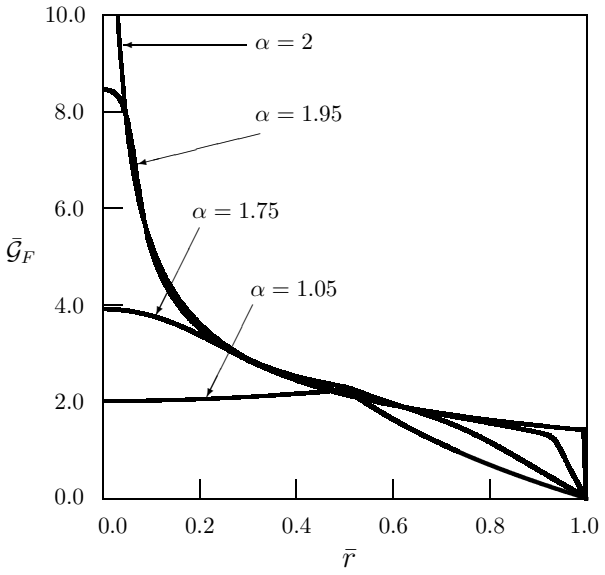

Figure 5.24: The fundamental solution to the second Cauchy problem in a cylinder under zero Dirichlet boundary condition ($\bar{\rho} = 0.5$, $\kappa = 0.5$)

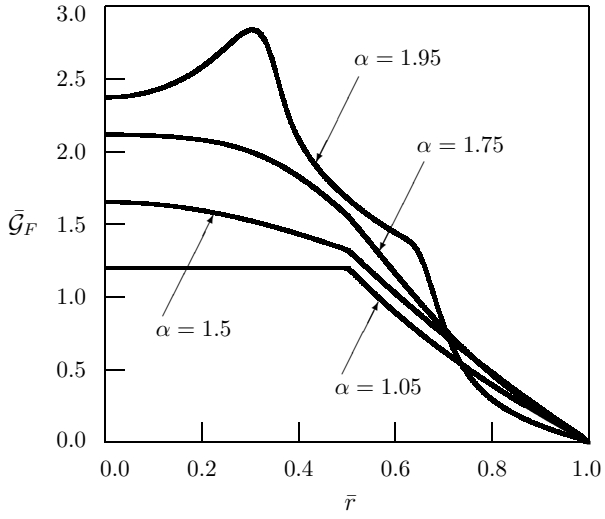

Figure 5.25: The fundamental solution to the second Cauchy problem in a cylinder under zero Dirichlet boundary condition ($\bar{\rho} = 0.5$, $\kappa = 0.75$)

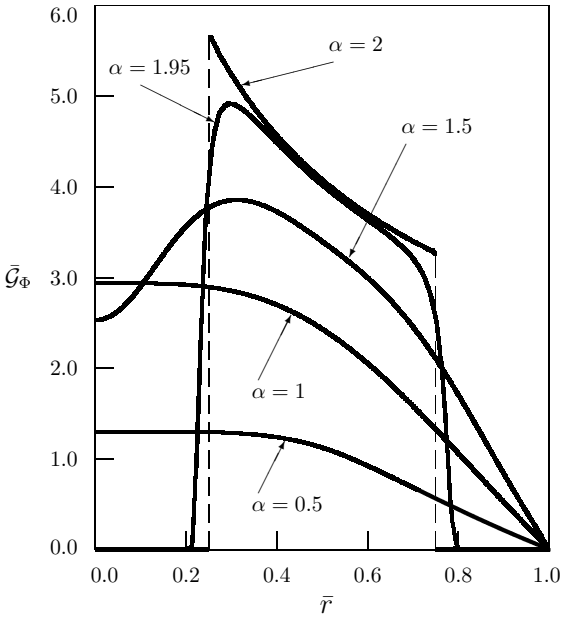

Figure 5.26: The fundamental solution to the source problem in a cylinder under zero Dirichlet boundary condition ($\bar{\rho} = 0.5$, $\kappa = 0.25$)

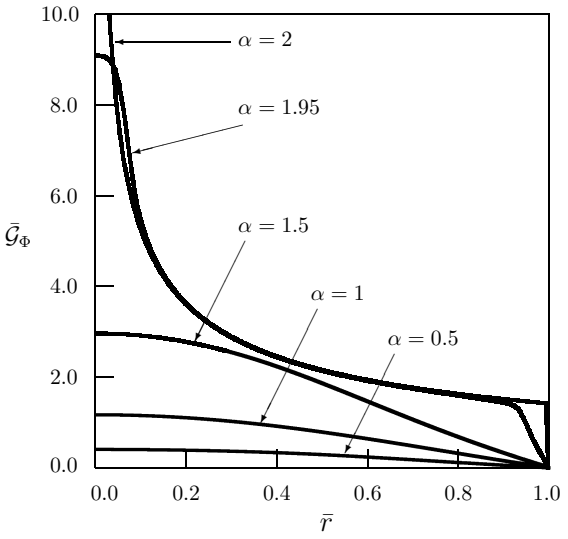

Figure 5.27: The fundamental solution to the source problem in a cylinder under zero Dirichlet boundary condition ($\bar{\rho} = 0.5$, $\kappa = 0.5$)

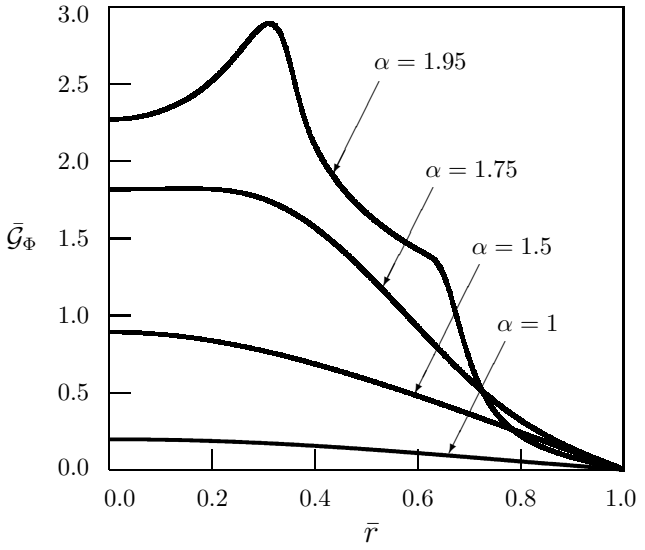

Figure 5.28: The fundamental solution to the source problem in a cylinder under zero Dirichlet boundary condition ($\bar{\rho} = 0.5$, $\kappa = 0.75$)

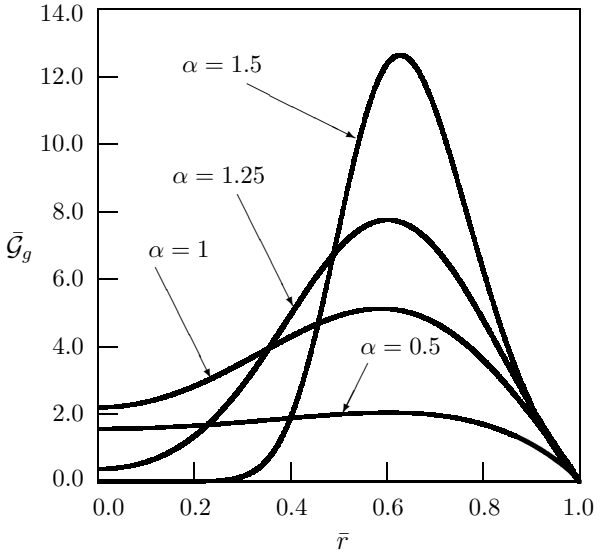

Figure 5.29: The fundamental solution to the Dirichlet problem in a cylinder; $\kappa = 0.25$

Constant source strength. Here we consider the fractional diffusion-wave equation with constant source term $Q_0 = \text{const}$

$$\frac{\partial^\alpha T}{\partial t^\alpha} = a\left(\frac{\partial^2 T}{\partial r^2} + \frac{1}{r}\frac{\partial T}{\partial r}\right) + Q_0 \tag{5.75}$$

under zero initial conditions

$$t = 0: \quad T = 0, \qquad 0 < \alpha \le 2, \tag{5.76}$$

$$t = 0: \quad \frac{\partial T}{\partial t} = 0, \qquad 1 < \alpha \le 2, \tag{5.77}$$

and zero Dirichlet boundary condition

$$r = R: \quad T = 0, \tag{5.78}$$

having the solution [149]

$$T = \frac{Q_0}{4a}\left(R^2 - r^2\right) - \frac{2Q_0}{aR}\sum_{k=1}^{\infty} E_\alpha\left(-a\xi_k^2 t^\alpha\right)\frac{J_0(r\xi_k)}{\xi_k^3 J_1(R\xi_k)}. \tag{5.79}$$

Helmholtz equation ($\alpha \to 0$)

$$T = \frac{Q_0}{4a}\left(R^2 - r^2\right) - \frac{2Q_0}{aR}\sum_{k=1}^{\infty} \frac{1}{1 + a\xi_k^2}\frac{J_0(r\xi_k)}{\xi_k^3 J_1(R\xi_k)}. \tag{5.80}$$

Classical diffusion equation ($\alpha = 1$)

$$T = \frac{Q_0}{4a}\left(R^2 - r^2\right) - \frac{2Q_0}{aR}\sum_{k=1}^{\infty} \exp\left(-a\xi_k^2 t\right)\frac{J_0(r\xi_k)}{\xi_k^3 J_1(R\xi_k)}. \tag{5.81}$$

The solution (5.81) is presented in [26].

Wave equation ($\alpha = 2$)

$$T = \frac{Q_0}{4a}\left(R^2 - r^2\right) - \frac{2Q_0}{aR}\sum_{k=1}^{\infty} \cos\left(\sqrt{a}\xi_k t\right)\frac{J_0(r\xi_k)}{\xi_k^3 J_1(R\xi_k)}. \tag{5.82}$$

The results of numerical calculations are shown in Figs. 5.30 and 5.31 with $\overline{T} = aT/(Q_0 R^2)$.

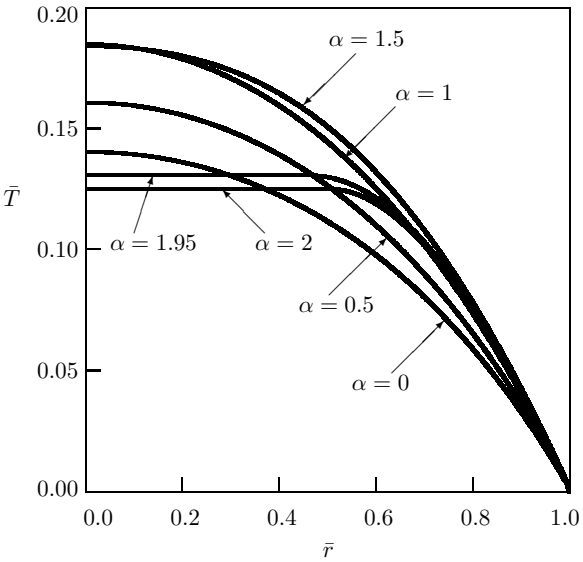

Figure 5.30: Dependence of temperature in a cylinder on distance (the constant source strength; $\kappa = 0.5$ [149]

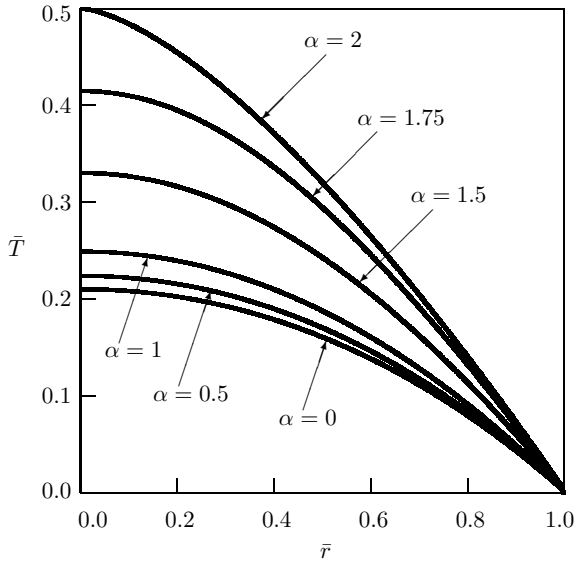

Figure 5.31: Dependence of temperature in a cylinder on distance (the constant source strength; $\kappa = 1$ [149]

Dirichlet problem with constant boundary condition

$$\frac{\partial^\alpha T}{\partial t^\alpha} = a\left(\frac{\partial^2 T}{\partial r^2} + \frac{1}{r}\,\frac{\partial T}{\partial r}\right), \tag{5.83}$$

$$t = 0: \quad T = 0, \qquad 0 < \alpha \le 2, \tag{5.84}$$

$$t = 0: \quad \frac{\partial T}{\partial t} = 0, \qquad 1 < \alpha \le 2, \tag{5.85}$$

$$r = R: \quad T = T_0. \tag{5.86}$$

The solution has the form:

$$T = T_0\left[1 - 2\sum_{k=1}^{\infty} E_\alpha\left(-a\xi_k^2 t^\alpha\right)\frac{J_0(r\xi_k)}{R\xi_k\, J_1(R\xi_k)}\right]. \tag{5.87}$$

The solution (5.87) was obtained by Narahari Achar and Hanneken [126], but their numerical analysis of this solution and conclusions from such an analysis need improvement (see [149]). The results of numerical calculations according to (5.87) are presented in Figs. 5.32–5.34 for typical values of the parameter κ with $(\overline{T} = T/T_0)$.

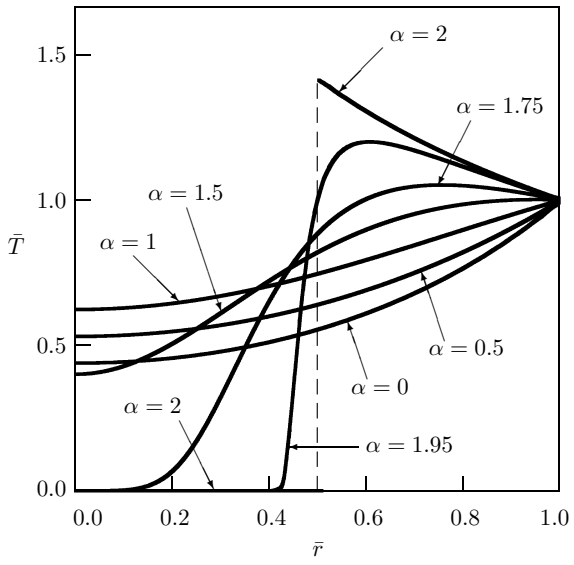

Figure 5.32: Dependence of temperature in a cylinder on distance (the constant boundary condition; $\kappa = 0.5$ [149]

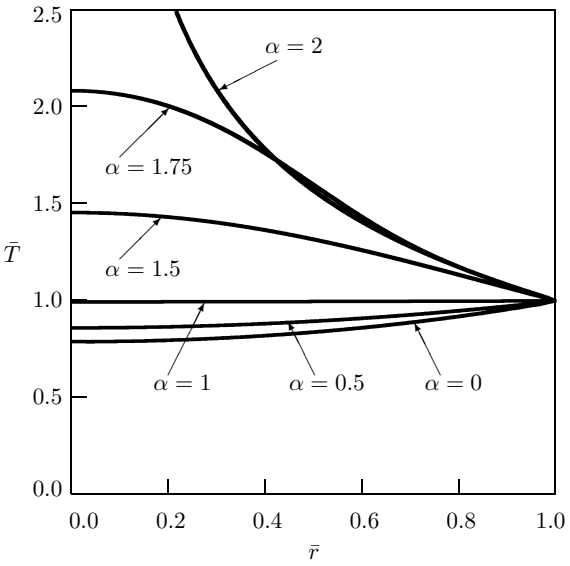

Figure 5.33: Dependence of temperature in a cylinder on distance (the constant boundary condition; $\kappa = 1$ [149]

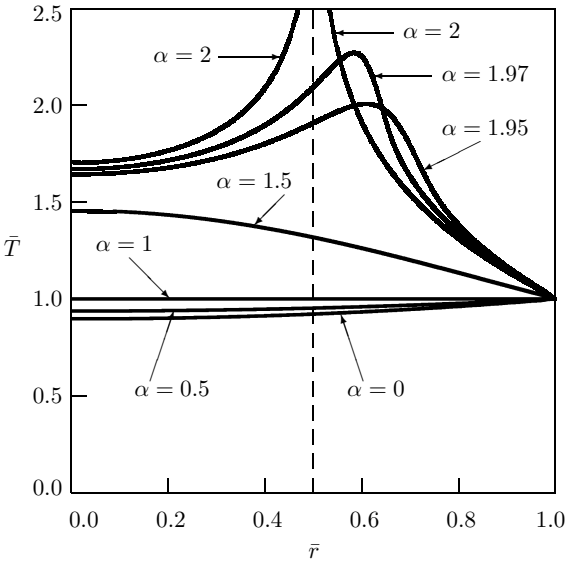

Figure 5.34: Dependence of temperature in a cylinder on distance (the constant boundary condition; $\kappa = 1.5$ [149]

5.3.2 Neumann boundary condition

$$\frac{\partial^\alpha T}{\partial t^\alpha} = a\left(\frac{\partial^2 T}{\partial r^2} + \frac{1}{r}\,\frac{\partial T}{\partial r}\right) + \Phi(r,t), \tag{5.88}$$

$$t = 0: \quad T = f(r), \qquad 0 < \alpha \le 2, \tag{5.89}$$

$$t = 0: \quad \frac{\partial T}{\partial t} = F(r), \quad 1 < \alpha \le 2, \tag{5.90}$$

$$r = R: \quad \frac{\partial T}{\partial r} = g(t). \tag{5.91}$$

The solution:

$$T(r,t) = \int_0^R f(\rho)\,\mathcal{G}_f(r,\rho,t)\,\rho\,\mathrm{d}\rho + \int_0^R F(\rho)\,\mathcal{G}_F(r,\rho,t)\,\rho\,\mathrm{d}\rho$$
$$+ \int_0^t \int_0^R \Phi(\rho,\tau)\,\mathcal{G}_\Phi(r,\rho,t-\tau)\,\rho\,\mathrm{d}\rho\,\mathrm{d}\tau + \int_0^t g(\tau)\,\mathcal{G}_g(r,t-\tau)\,\mathrm{d}\tau. \tag{5.92}$$

The fundamental solutions under zero Neumann boundary condition have the form

$$\begin{pmatrix} \mathcal{G}_f(r,\rho,t) \\ \mathcal{G}_F(r,\rho,t) \\ \mathcal{G}_\Phi(r,\rho,t) \end{pmatrix} = \frac{2}{R^2}\begin{pmatrix} p_0 \\ w_0 t \\ q_0 t^{\alpha-1}/\Gamma(\alpha) \end{pmatrix}$$

$$+\frac{2}{R^2}\sum_{k=1}^{\infty}\begin{pmatrix} p_0\,E_\alpha(-a\xi_k^2 t^\alpha) \\ w_0 t\,E_{\alpha,2}(-a\xi_k^2 t^\alpha) \\ q_0 t^{\alpha-1}\,E_{\alpha,\alpha}(-a\xi_k^2 t^\alpha) \end{pmatrix}\frac{J_0(r\xi_k)J_0(\rho\xi_k)}{J_0^2(R\xi_k)}, \tag{5.93}$$

with sum over all positive roots of the first-order Bessel function

$$J_1(R\xi_k) = 0. \tag{5.94}$$

The solutions were obtained using the Laplace transform with respect to time and the finite Hankel transform (2.100) with respect to the radial coordinate.

Dependence of the fundamental solution $\overline{\mathcal{G}}_f$ on nondimensional distance r is shown in Figs. 5.35–5.36. Dependence of the fundamental solution $\overline{\mathcal{G}}_F$ on distance is presented in Figs. 5.37–5.39. Dependence of the fundamental solution $\overline{\mathcal{G}}_\Phi$ on distance is depicted in Figs. 5.40–5.42. The nondimensional quantities are the same as in (5.74). For $\kappa = 0.25$ the fundamental solutions under zero Dirichlet and Neumann boundary conditions behave very similarly (the solutions do not "feel" the boundary condition), but for $\kappa = 0.5$ and $\kappa = 0.75$ there appears significant difference.

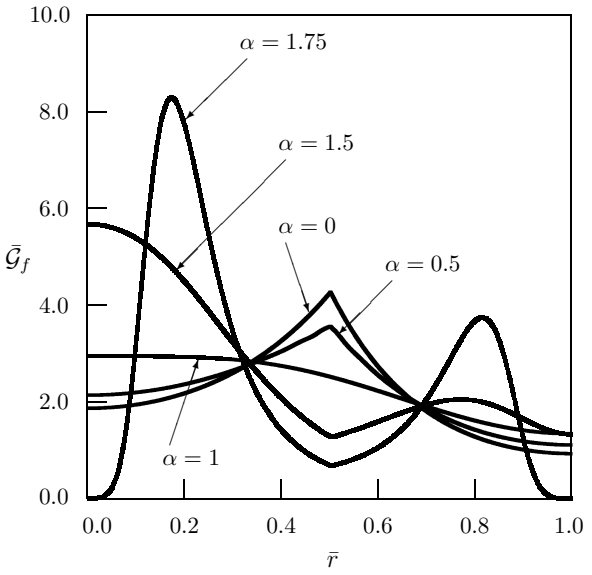

Figure 5.35: The fundamental solution to the first Cauchy problem in a cylinder under zero Neumann boundary condition ($\bar{\rho} = 0.5$, $\kappa = 0.25$)

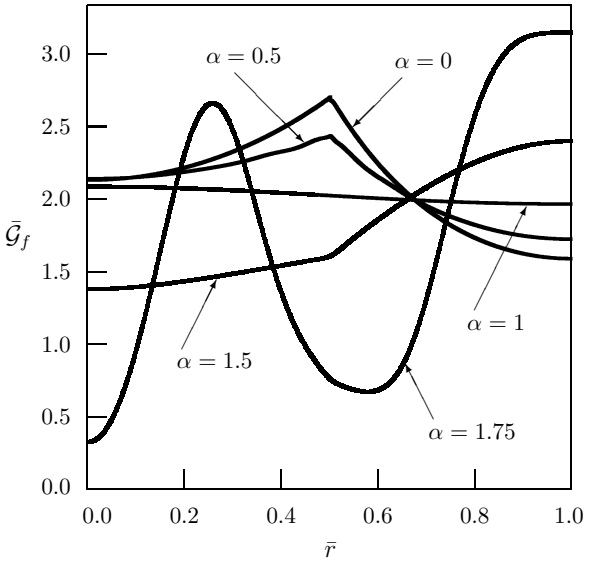

Figure 5.36: The fundamental solution to the first Cauchy problem in a cylinder under zero Neumann boundary condition ($\bar{\rho} = 0.5$, $\kappa = 0.5$)

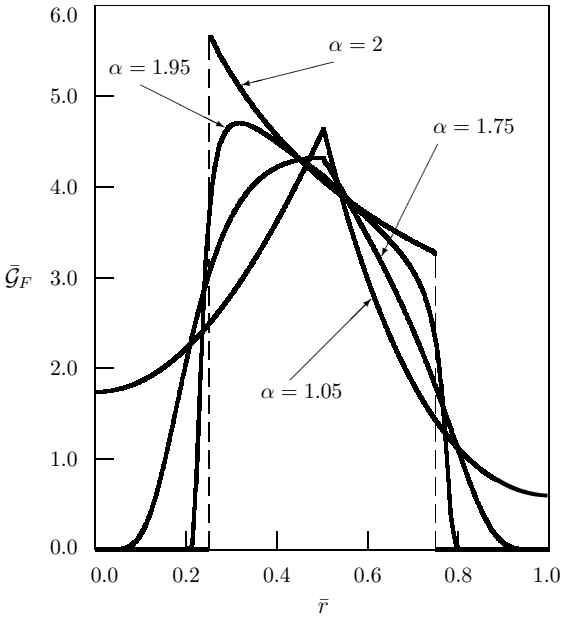

Figure 5.37: The fundamental solution to the second Cauchy problem in a cylinder under zero Neumann boundary condition ($\bar{\rho} = 0.5$, $\kappa = 0.25$)

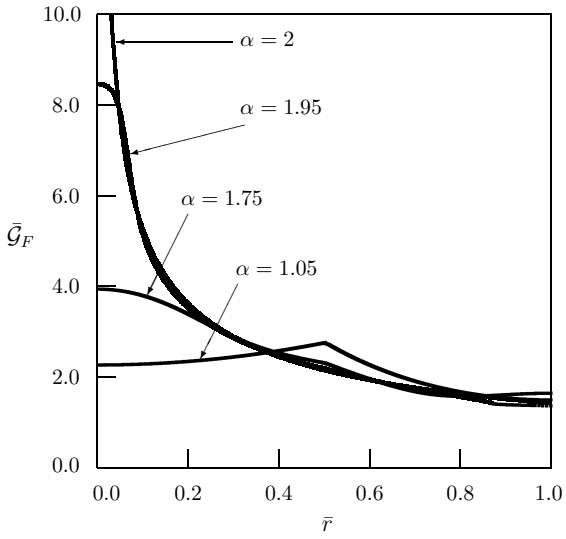

Figure 5.38: The fundamental solution to the second Cauchy problem in a cylinder under zero Neumann boundary condition ($\bar{\rho} = 0.5$, $\kappa = 0.5$)

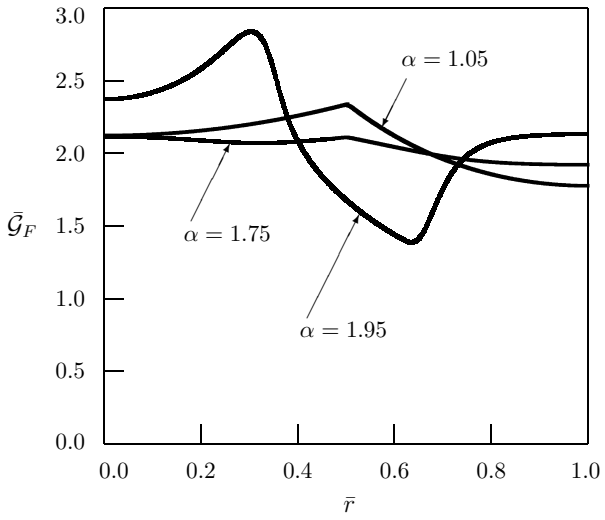

Figure 5.39: The fundamental solution to the second Cauchy problem in a cylinder under zero Neumann boundary condition ($\bar{\rho} = 0.5$, $\kappa = 0.75$)

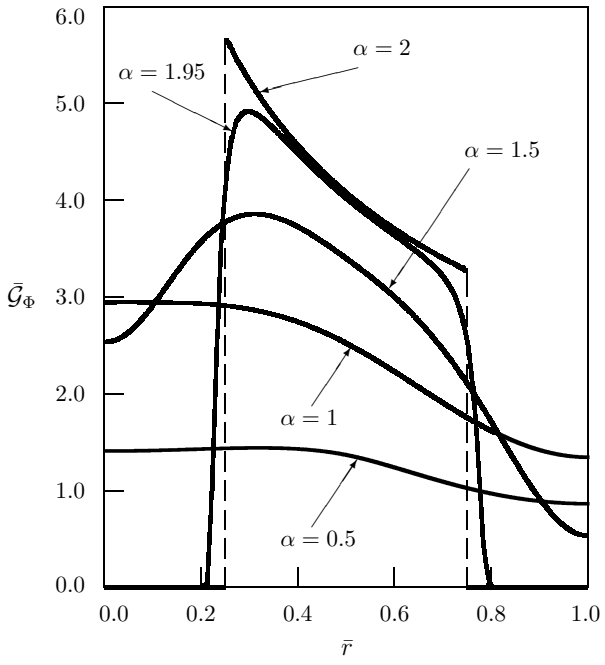

Figure 5.40: The fundamental solution to the source problem in a cylinder under zero Neumann boundary condition ($\bar{\rho} = 0.5$, $\kappa = 0.25$)

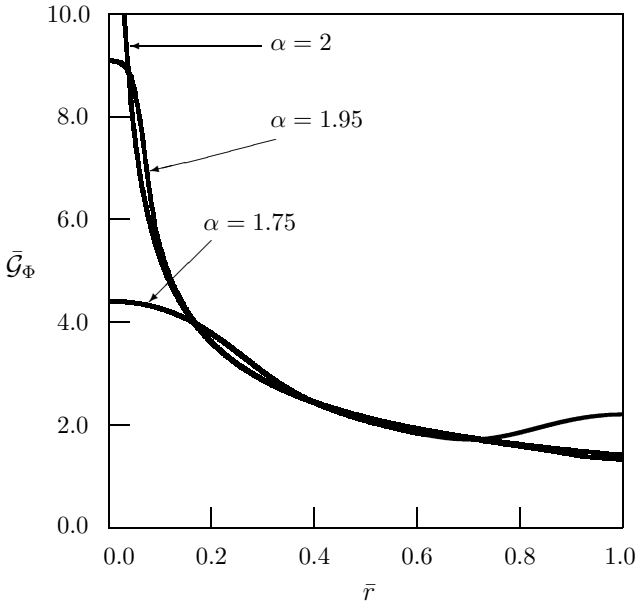

Figure 5.41: The fundamental solution to the source problem in a cylinder under zero Neumann boundary condition ($\bar{\rho} = 0.5$, $\kappa = 0.5$)

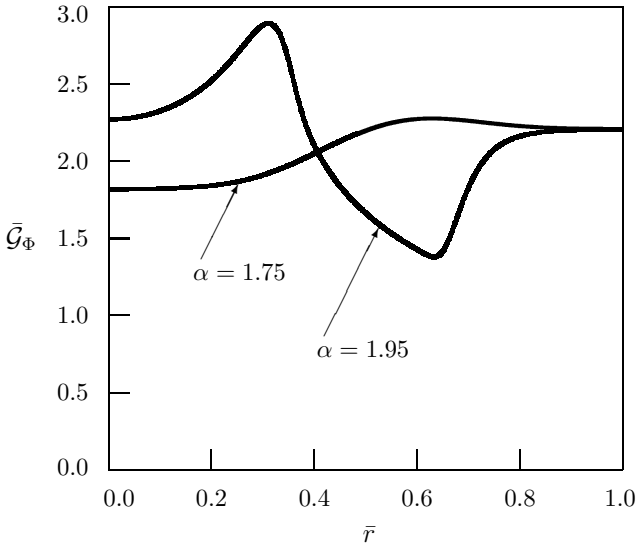

Figure 5.42: The fundamental solution to the source problem in a cylinder under zero Neumann boundary condition ($\bar{\rho} = 0.5$, $\kappa = 0.75$)

Fundamental solution to the mathematical Neumann problem

$$\frac{\partial^\alpha \mathcal{G}_m}{\partial t^\alpha} = a\left(\frac{\partial^2 \mathcal{G}_m}{\partial r^2} + \frac{1}{r}\,\frac{\partial \mathcal{G}_m}{\partial r}\right), \tag{5.95}$$

$$t = 0: \quad \mathcal{G}_m = 0, \qquad 0 < \alpha \le 2, \tag{5.96}$$

$$t = 0: \quad \frac{\partial \mathcal{G}_m}{\partial t} = 0, \qquad 1 < \alpha \le 2, \tag{5.97}$$

$$r = R: \quad \frac{\partial \mathcal{G}_m}{\partial r} = g_0\,\delta(t). \tag{5.98}$$

The solution reads:

$$\mathcal{G}_m(r,t) = \frac{2ag_0 t^{\alpha-1}}{R}\left[\frac{1}{\Gamma(\alpha)} + \sum_{k=1}^{\infty} E_{\alpha,\alpha}\left(-a\xi_k^2 t^\alpha\right)\frac{J_0(r\xi_k)}{J_0(R\xi_k)}\right]. \tag{5.99}$$

The solution (5.99) is shown in Figs. 5.43 and 5.44, where $\overline{\mathcal{G}}_m = Rt^{1-\alpha}\mathcal{G}_m/(ag_0)$.

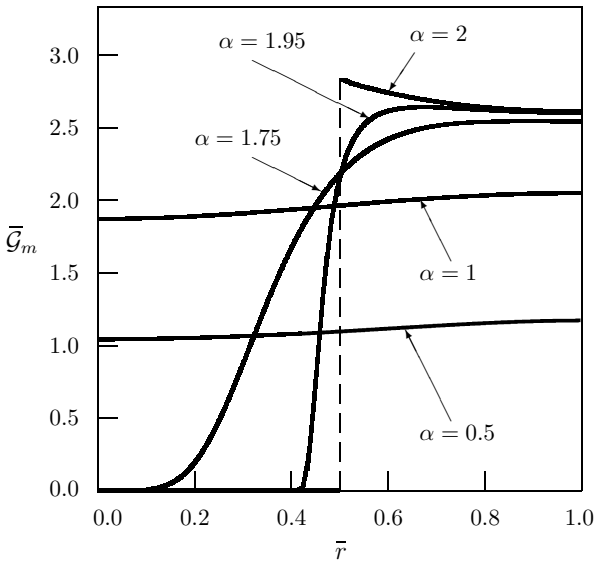

Figure 5.43: The fundamental solution to the mathematical Neumann problem for a cylinder; $\kappa = 0.5$

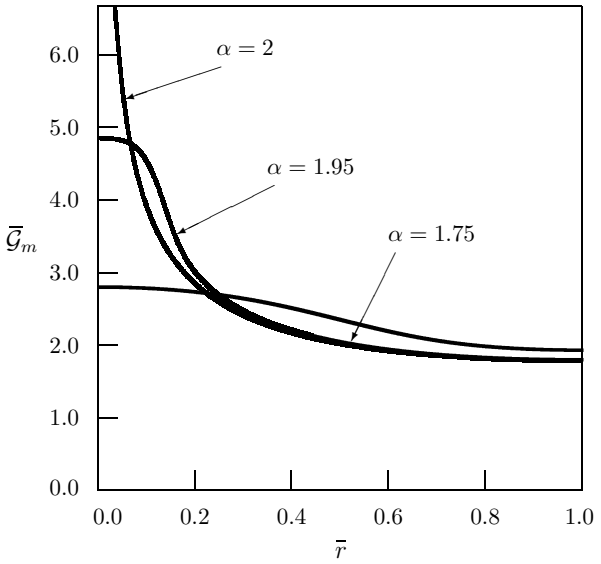

Figure 5.44: The fundamental solution to the mathematical Neumann problem for a cylinder; $\kappa = 1$

Constant boundary value of the normal derivative. In the case when a constant boundary value of the normal derivative is considered,

$$r = R: \quad \frac{\partial T}{\partial r} = g_0, \tag{5.100}$$

the solution has the following form [174]:

$$T = \frac{2ag_0 t^\alpha}{R\Gamma(1+\alpha)} + \frac{g_0}{R}\left[\frac{r^2}{2} - \frac{R^2}{4} - 2\sum_{k=1}^{\infty} E_\alpha\left(-a\xi_k^2 t^\alpha\right)\frac{J_0(r\xi_k)}{\xi_k^2\, J_0(R\xi_k)}\right]. \tag{5.101}$$

The particular case of (5.101) corresponding to the classical diffusion equation ($\alpha = 1$) coincides with the corresponding solution presented in [26].

The results of numerical calculations are presented in Fig. 5.45 and Fig. 5.46 with $\overline{T} = T/(g_0 R)$.

Fundamental solution to the physical Neumann problem

$$\frac{\partial^\alpha \mathcal{G}_p}{\partial t^\alpha} = a\left(\frac{\partial^2 \mathcal{G}_p}{\partial r^2} + \frac{1}{r}\frac{\partial \mathcal{G}_p}{\partial r}\right), \tag{5.102}$$

$$t = 0: \quad \mathcal{G}_p = 0, \qquad 0 < \alpha \le 2, \tag{5.103}$$

$$t = 0: \quad \frac{\partial \mathcal{G}_p}{\partial t} = 0, \qquad 1 < \alpha \le 2, \tag{5.104}$$

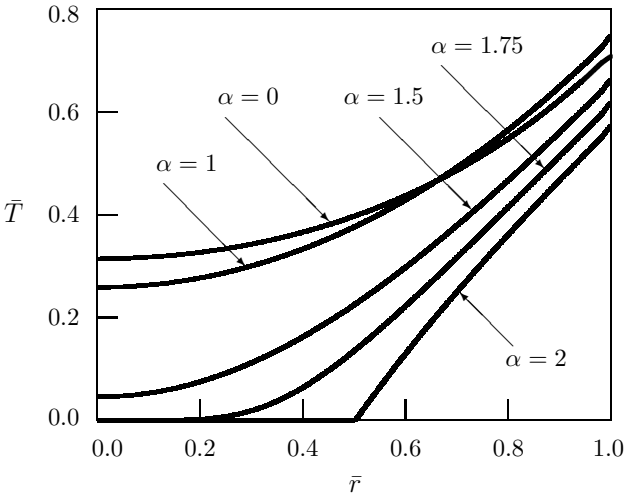

Figure 5.45: Dependence of temperature in a cylinder on distance (the constant normal derivative of temperature at the boundary; $\kappa = 0.5$)

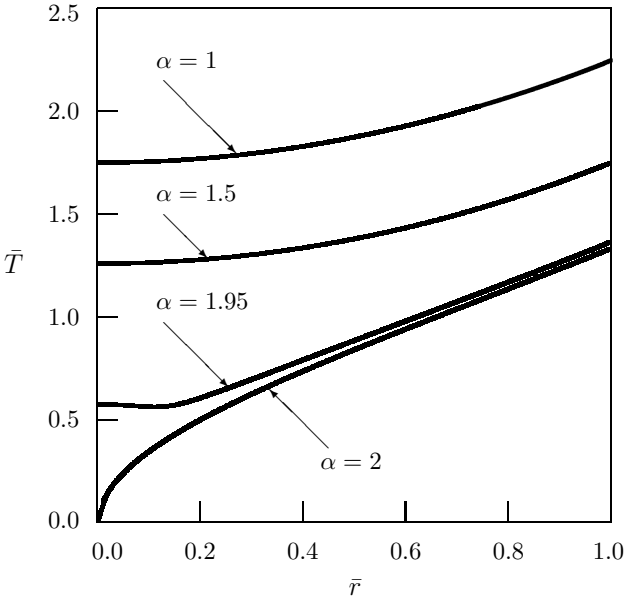

Figure 5.46: Dependence of temperature in a cylinder on distance (the constant normal derivative of temperature at the boundary; $\kappa = 1$)

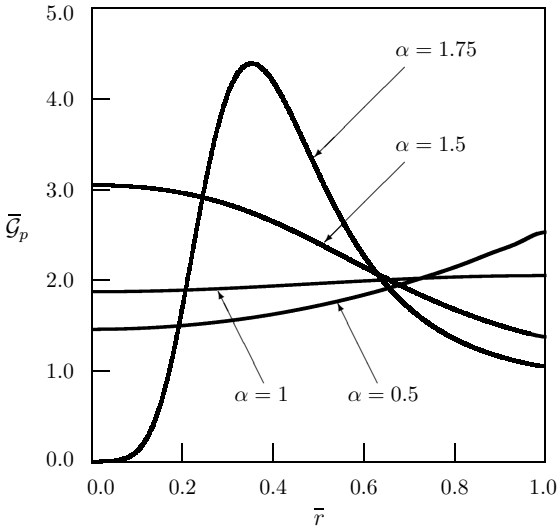

Figure 5.47: The fundamental solution to the physical Neumann problem for a cylinder; $\kappa = 0.5$

$$r = R: \quad D_{RL}^{1-\alpha} \frac{\partial \mathcal{G}_p}{\partial r} = g_0\, \delta(t), \qquad 0 < \alpha \le 1, \tag{5.105}$$

$$r = R: \quad I^{\alpha-1} \frac{\partial \mathcal{G}_p}{\partial r} = g_0\, \delta(t), \qquad 1 < \alpha \le 2. \tag{5.106}$$

The solution

$$\mathcal{G}_p(r,t) = \frac{2ag_0}{R} \left[1 + \sum_{k=1}^{\infty} E_\alpha \left(-a\xi_k^2 t^\alpha \right) \frac{J_0(r\xi_k)}{J_0(R\xi_k)} \right] \tag{5.107}$$

is shown in Figs. 5.47 and 5.48 with $\overline{\mathcal{G}}_p = R\mathcal{G}_p/(ag_0)$.

Constant heat flux at the boundary

$$\frac{\partial^\alpha T}{\partial t^\alpha} = a \left(\frac{\partial^2 T}{\partial r^2} + \frac{1}{r} \frac{\partial T}{\partial r} \right) \tag{5.108}$$

$$t = 0: \quad T = 0, \qquad 0 < \alpha \le 2, \tag{5.109}$$

$$t = 0: \quad \frac{\partial T}{\partial t} = 0, \qquad 1 < \alpha \le 2, \tag{5.110}$$

$$r = R: \quad D_{RL}^{1-\alpha} \frac{\partial T}{\partial r} = g_0, \quad 0 < \alpha \le 1, \tag{5.111}$$

$$r = R: \quad I^{\alpha-1} \frac{\partial T}{\partial r} = g_0, \quad 1 < \alpha \le 2. \tag{5.112}$$

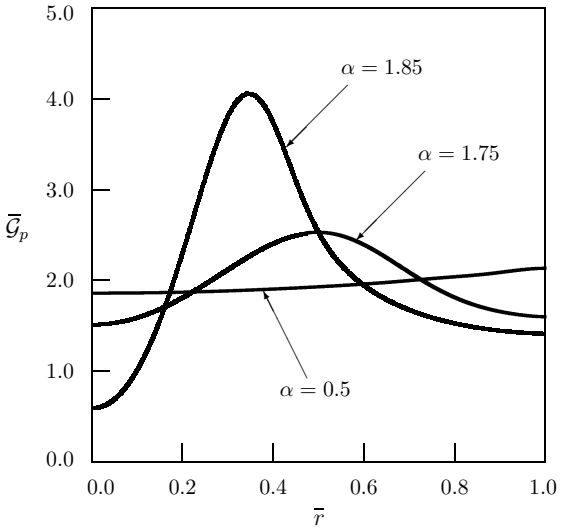

Figure 5.48: The fundamental solution to the physical Neumann problem for a cylinder; $\kappa = 1$

The solution [174]:

$$T = \frac{2ag_0t}{R}\left[1 + \sum_{k=1}^{\infty} E_{\alpha,2}\left(-a\xi_k^2 t^\alpha\right)\frac{J_0(r\xi_k)}{J_0(R\xi_k)}\right]. \tag{5.113}$$

The results of numerical calculations of the solution (5.113) are presented in Fig. 5.49 and Fig. 5.50 with $\overline{T} = t^{\alpha-1}T/(g_0R)$.

5.3.3 Robin boundary condition

$$\frac{\partial^\alpha T}{\partial t^\alpha} = a\left(\frac{\partial^2 T}{\partial r^2} + \frac{1}{r}\frac{\partial T}{\partial r}\right) + \Phi(r,t), \tag{5.114}$$

$$t = 0: \quad T = f(r), \qquad 0 < \alpha \le 2, \tag{5.115}$$

$$t = 0: \quad \frac{\partial T}{\partial t} = F(r), \quad 1 < \alpha \le 2, \tag{5.116}$$

$$r = R: \quad HT + \frac{\partial T}{\partial t} = g(t). \tag{5.117}$$

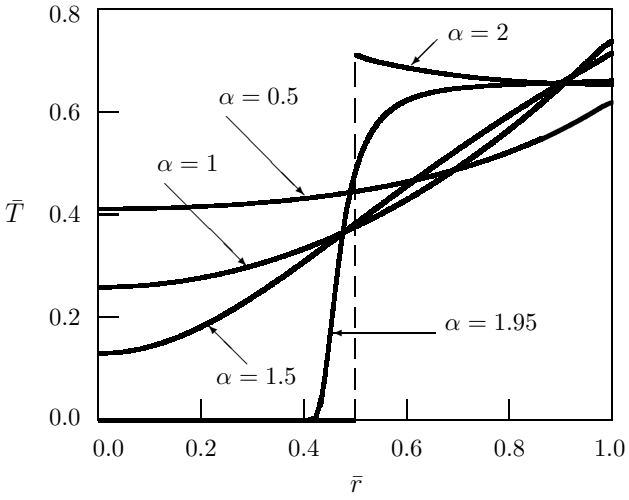

Figure 5.49: Dependence of temperature in a cylinder on distance (the constant heat flux at the boundary; $\kappa = 0.5$)

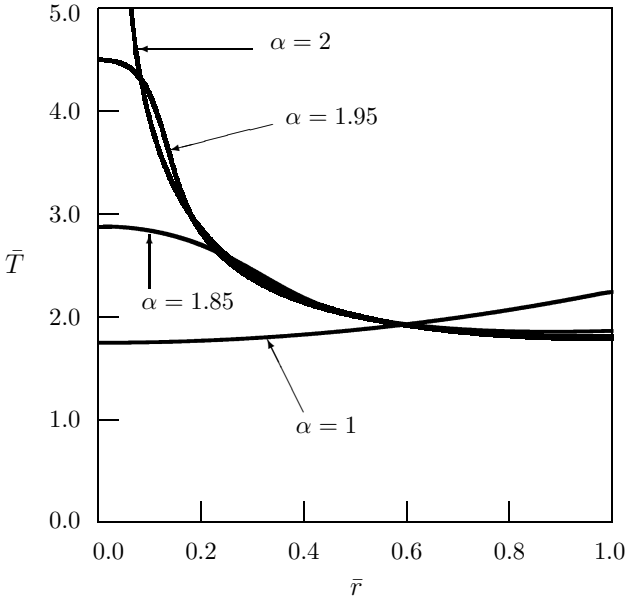

Figure 5.50: Dependence of temperature in a cylinder on distance (the constant heat flux at the boundary; $\kappa = 1$

The solution:

$$T(r,t) = \int_0^R f(\rho)\,\mathcal{G}_f(r,\rho,t)\,\rho\,\mathrm{d}\rho + \int_0^R F(\rho)\,\mathcal{G}_F(r,\rho,t)\,\rho\,\mathrm{d}\rho + \int_0^t \int_0^R \Phi(\rho,\tau)\,\mathcal{G}_\Phi(r,\rho,t-\tau)\,\rho\,\mathrm{d}\rho\,\mathrm{d}\tau + \int_0^t g(\tau)\,\mathcal{G}_g(r,t-\tau)\,\mathrm{d}\tau. \tag{5.118}$$

The fundamental solutions [186]

$$\begin{pmatrix} \mathcal{G}_f(r,\rho,t) \\ \mathcal{G}_F(r,\rho,t) \\ \mathcal{G}_\Phi(r,\rho,t) \end{pmatrix} = \frac{2}{R^2} \sum_{k=1}^{\infty} \begin{pmatrix} p_0\,E_\alpha(-a\xi_k^2 t^\alpha) \\ w_0 t\,E_{\alpha,2}(-a\xi_k^2 t^\alpha) \\ q_0 t^{\alpha-1}\,E_{\alpha,\alpha}(-a\xi_k^2 t^\alpha) \end{pmatrix} \times \frac{\xi_k^2}{\xi_k^2 + H^2}\,\frac{J_0(r\xi_k)J_0(\rho\xi_k)}{J_0^2(R\xi_k)} \tag{5.119}$$

with sum over all positive roots of the transcendental equation

$$\xi_k J_1(R\xi_k) = H J_0(R\xi_k) \tag{5.120}$$

are obtained using the Laplace transform with respect to time t and the finite Hankel transform (2.104) with respect to the radial coordinate r.

The fundamental solution to the mathematical Robin problem under zero initial condition is expressed as

$$\mathcal{G}_g(r,t) = \frac{aRg_0}{q_0}\,\mathcal{G}_\Phi(r,\rho,t)\Big|_{\rho=R}. \tag{5.121}$$

Dependence of the fundamental solution $\mathcal{G}_f$ on nondimensional distance r is shown in Figs. 5.51–5.52 ($\overline{H} = RH$, $\overline{\mathcal{G}}_f = R^2\mathcal{G}_f/p_0$). The fundamental solution $\mathcal{G}_F$ is depicted in Figs. 5.53–5.55 with $\overline{\mathcal{G}}_F = R^2\mathcal{G}_F/(w_0 t)$. The fundamental solution $\mathcal{G}_\Phi$ is presented in Figs. 5.56–5.58 for various values of α, κ and $\bar{H}$, where $\overline{\mathcal{G}}_\Phi = R^2 t^{1-\alpha}\mathcal{G}_\Phi/q_0$. The fundamental solution to the mathematical Robin boundary value problem under zero initial conditions $\mathcal{G}_g(r,t)$ is shown in Figs. 5.59 and 5.60 with $\overline{\mathcal{G}}_g = R\mathcal{G}_g T^{1-\alpha}/(ag_0)$. The fundamental solutions under Robin boundary conditions for $\kappa = 0.25$ do not "feel" the boundary condition, but for $\kappa = 0.5$ and $\kappa = 0.75$ there appears significant difference between solutions under Dirichlet, Neumann and Robin boundary conditions.

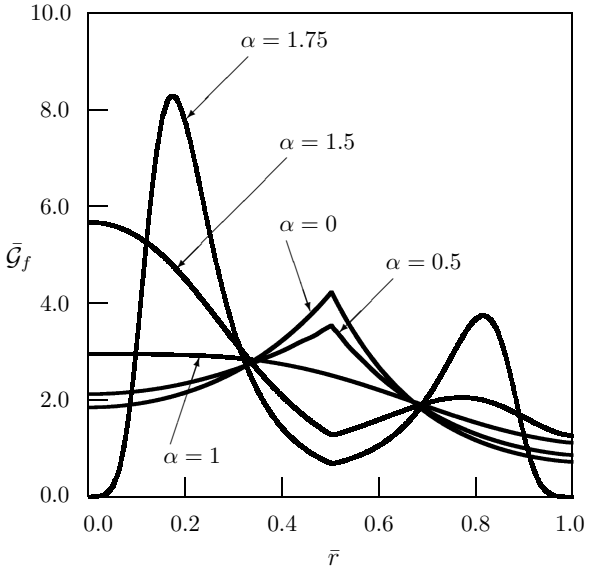

Figure 5.51: The fundamental solution to the first Cauchy problem in a cylinder under zero Robin boundary condition ($\bar{\rho} = 0.5$, $\kappa = 0.25$, $\bar{H} = 1$) [186]

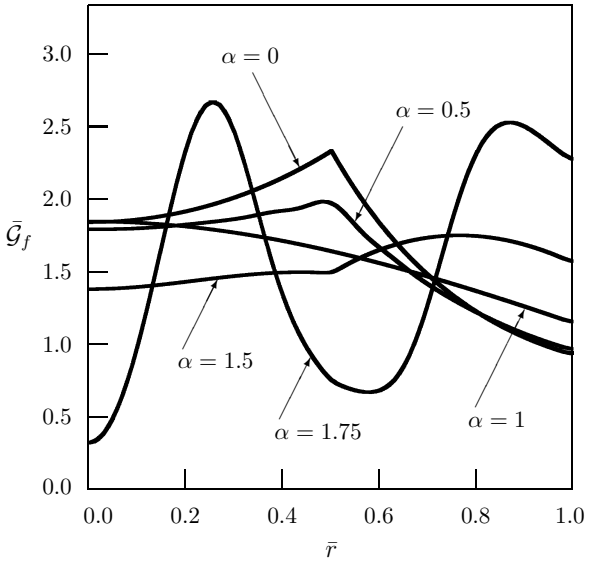

Figure 5.52: The fundamental solution to the first Cauchy problem in a cylinder under zero Robin boundary condition ($\bar{\rho} = 0.5$, $\kappa = 0.5$, $\bar{H} = 1$) [186]

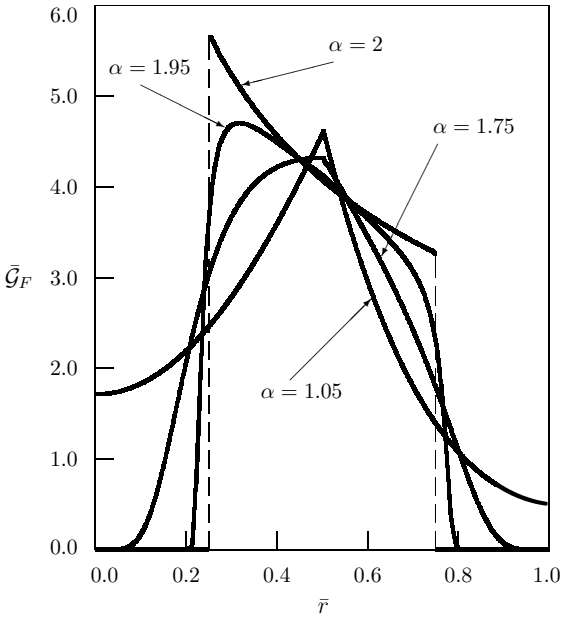

Figure 5.53: The fundamental solution to the second Cauchy problem in a cylinder under zero Robin boundary condition ($\bar{\rho} = 0.5$, $\kappa = 0.25$, $\bar{H} = 1$) [186]

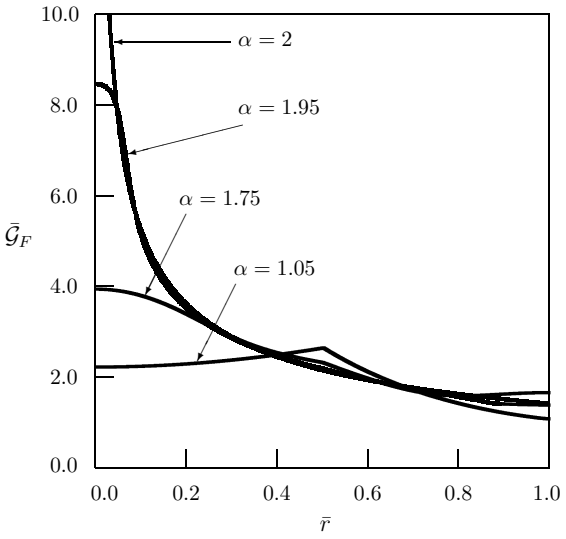

Figure 5.54: The fundamental solution to the second Cauchy problem in a cylinder under zero Robin boundary condition ($\bar{\rho} = 0.5$, $\kappa = 0.5$, $\bar{H} = 1$) [186]

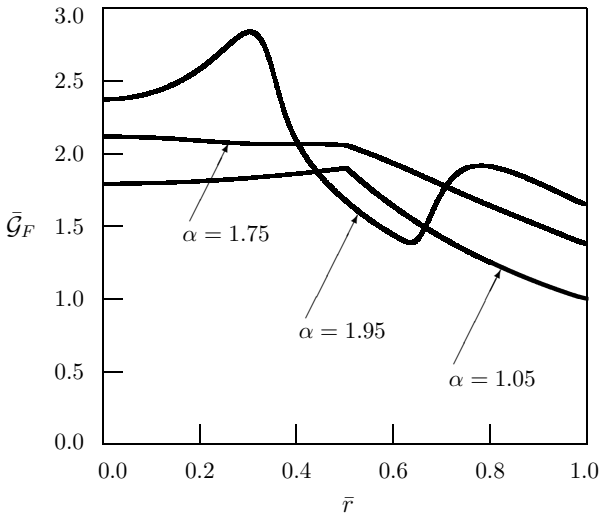

Figure 5.55: The fundamental solution to the second Cauchy problem in a cylinder under zero Robin boundary condition ($\bar{\rho} = 0.5$, $\kappa = 0.75$, $\bar{H} = 1$) [186]

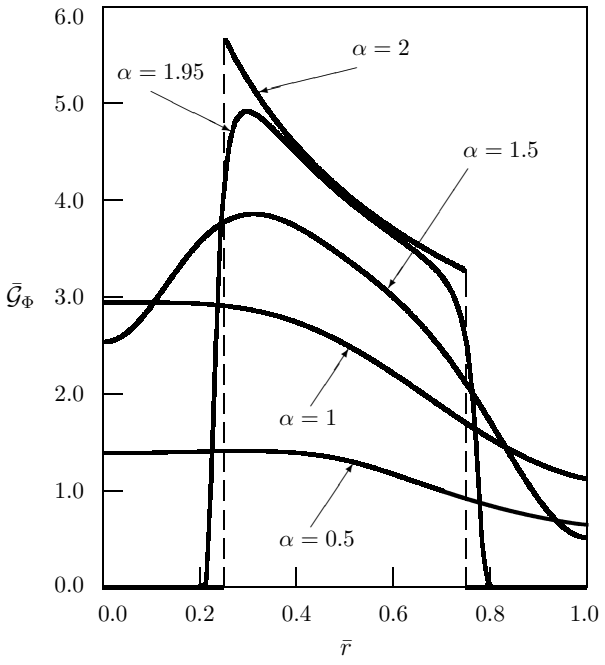

Figure 5.56: The fundamental solution to the source problem in a cylinder under zero Robin boundary condition ($\bar{\rho} = 0.5$, $\kappa = 0.25$, $\bar{H} = 1$) [186]

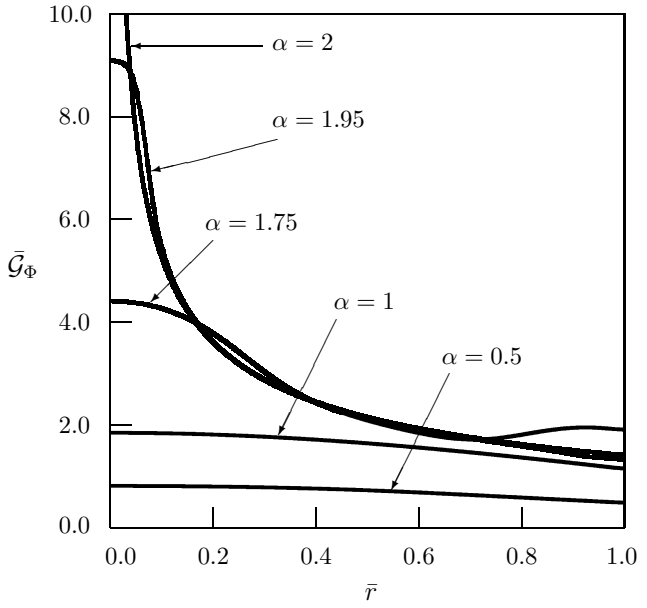

Figure 5.57: The fundamental solution to the source problem in a cylinder under zero Robin boundary condition ($\bar{\rho} = 0.5$, $\kappa = 0.5$, $\bar{H} = 1$) [186]

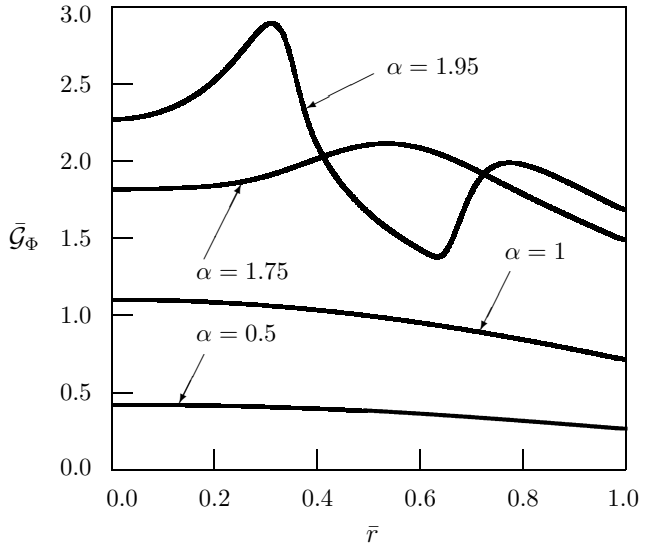

Figure 5.58: The fundamental solution to the source problem in a cylinder under zero Robin boundary condition ($\bar{\rho} = 0.5$, $\kappa = 0.75$, $\bar{H} = 1$) [186]

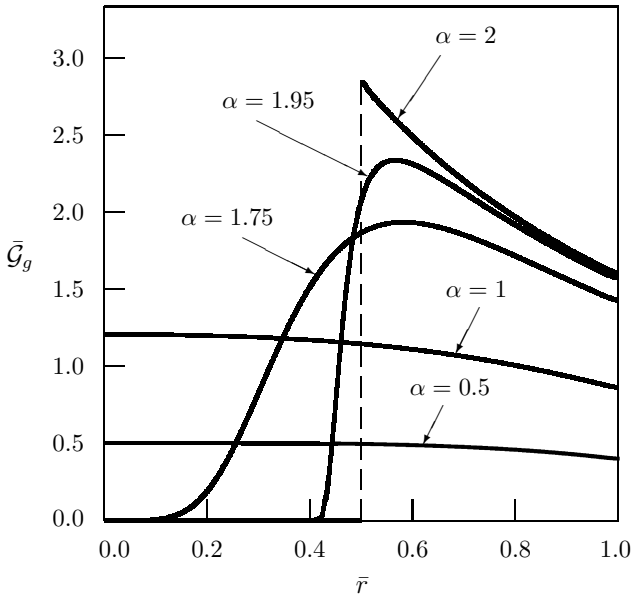

Figure 5.59: The fundamental solution to the Robin problem for a cylinder under zero initial conditions ($\kappa = 0.5$, $\bar{H} = 1$) [186]

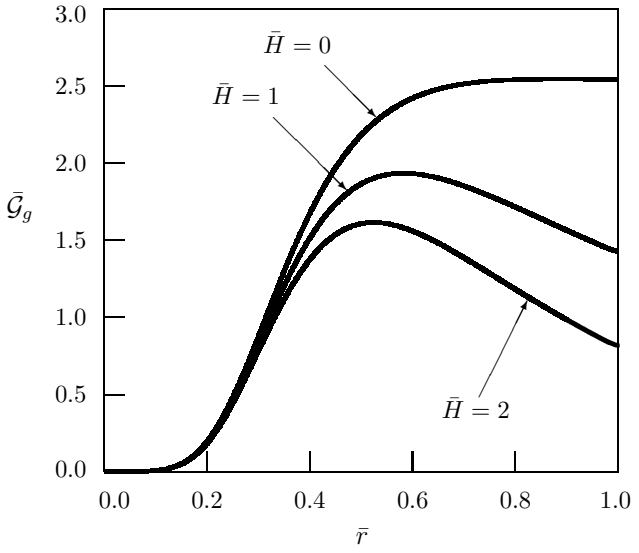

Figure 5.60: The fundamental solution to the Robin problem for a cylinder under zero initial conditions ($\alpha = 1.75$, $\kappa = 1$) [186]

5.4 Domain $R < r < \infty$

5.4.1 Dirichlet boundary condition

$$\frac{\partial^\alpha T}{\partial t^\alpha} = a\left(\frac{\partial^2 T}{\partial r^2} + \frac{1}{r}\,\frac{\partial T}{\partial r}\right) + \Phi(r,t), \tag{5.122}$$

$$t = 0: \quad T = f(r), \qquad 0 < \alpha \le 2, \tag{5.123}$$

$$t = 0: \quad \frac{\partial T}{\partial t} = F(r), \quad 1 < \alpha \le 2, \tag{5.124}$$

$$r = R: \quad T = g(t). \tag{5.125}$$

The zero condition at infinity is also assumed:

$$\lim_{r\to\infty} T(r,t) = 0. \tag{5.126}$$

The solution:

$$T(r,t) = \int\limits_R^\infty f(\rho)\,\mathcal{G}_f(r,\rho,t)\,\rho\,\mathrm{d}\rho + \int\limits_R^\infty F(\rho)\,\mathcal{G}_F(r,\rho,t)\,\rho\,\mathrm{d}\rho$$

$$+ \int\limits_0^t \int\limits_R^\infty \Phi(\rho,\tau)\,\mathcal{G}_\Phi(r,\rho,t-\tau)\,\rho\,\mathrm{d}\rho\,\mathrm{d}\tau + \int\limits_0^t g(\tau)\,\mathcal{G}_g(r,t-\tau)\,\mathrm{d}\tau. \tag{5.127}$$

The fundamental solutions under zero Dirichlet boundary condition,

$$\begin{pmatrix} \mathcal{G}_f(r,\rho,t) \\ \mathcal{G}_F(r,\rho,t) \\ \mathcal{G}_\Phi(r,\rho,t) \end{pmatrix} = \int\limits_0^\infty \begin{pmatrix} p_0\,E_\alpha(-a\xi^2 t^\alpha) \\ w_0 t\,E_{\alpha,2}(-a\xi^2 t^\alpha) \\ q_0 t^{\alpha-1}\,E_{\alpha,\alpha}(-a\xi^2 t^\alpha) \end{pmatrix} \frac{J_0(r\xi)\,Y_0(R\xi) - Y_0(r\xi)\,J_0(R\xi)}{J_0^2(R\xi) + Y_0^2(R\xi)}$$

$$\times \Big[J_0(\rho\xi)\,Y_0(R\xi) - Y_0(\rho\xi)\,J_0(R\xi)\Big]\,\xi\,\mathrm{d}\xi, \tag{5.128}$$

are obtained using the Laplace transform with respect to time t and the Weber transform (2.108), (2.117) with respect to the radial coordinate r.

Dependence of the fundamental solution $\bar{\mathcal{G}}_f = R^2\mathcal{G}_f/p_0$ on nondimensional distance $\bar{r} = r/R$ with $\bar{\rho} = \rho/R$ and $\kappa = \sqrt{a}t^\alpha/R$ is shown in Fig. 5.61. The fundamental solution $\bar{\mathcal{G}}_F = R^2\mathcal{G}_F/(w_0 t)$ is presented in Figs. 5.62 and 5.63. The fundamental solution to the source problem under zero Dirichlet boundary condition $\bar{\mathcal{G}}_\Phi = R^2\mathcal{G}_\Phi/(q_0 t^{\alpha-1})$ is depicted in Figs. 5.64 and 5.65.

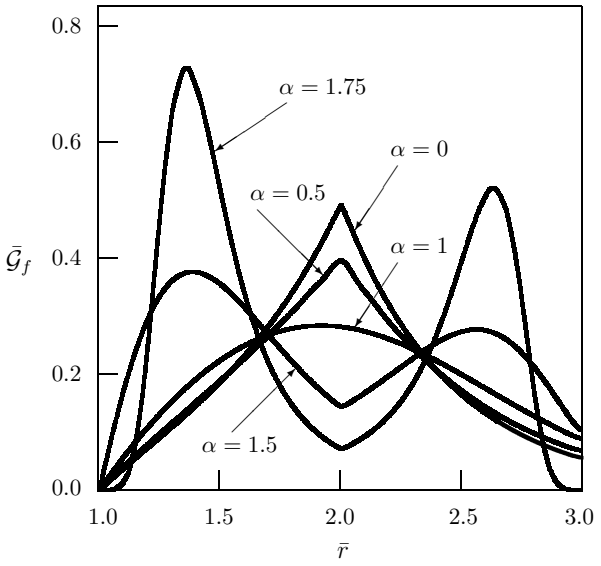

Figure 5.61: The fundamental solution to the first Cauchy problem in a body with a cylindrical hole under zero Dirichlet boundary condition ($\bar{\rho} = 2$, $\kappa = 0.5$)

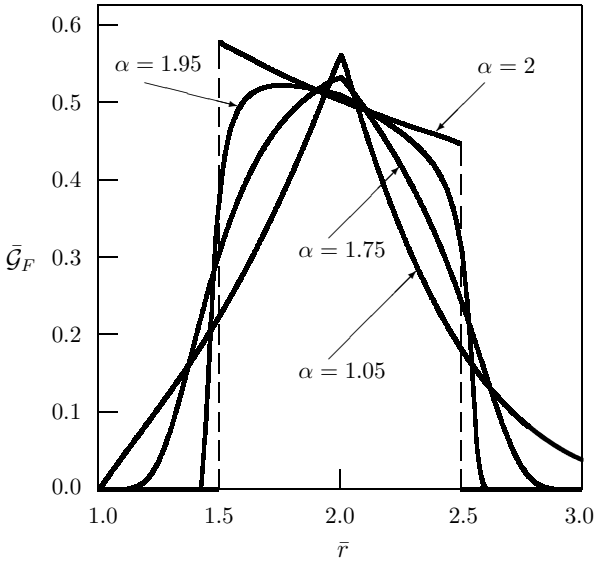

Figure 5.62: The fundamental solution to the second Cauchy problem in a body with a cylindrical hole under zero Dirichlet boundary condition ($\bar{\rho} = 2$, $\kappa = 0.5$)

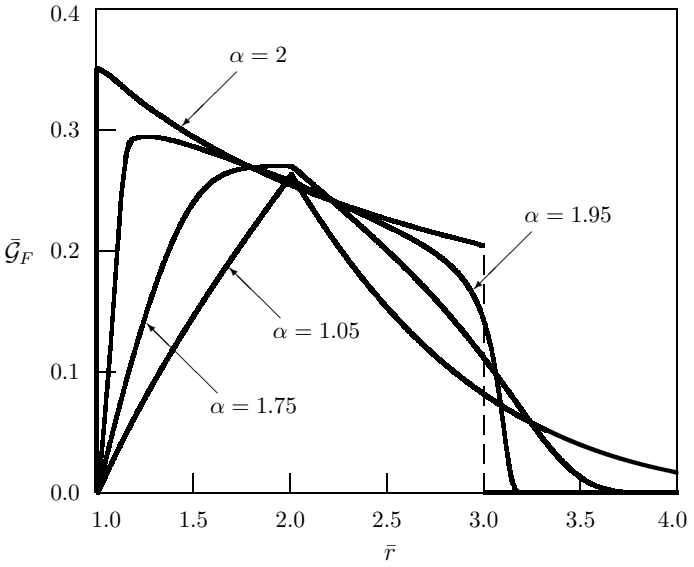

Figure 5.63: The fundamental solution to the second Cauchy problem in a body with a cylindrical hole under zero Dirichlet boundary condition ($\bar{\rho} = 2$, $\kappa = 1$)

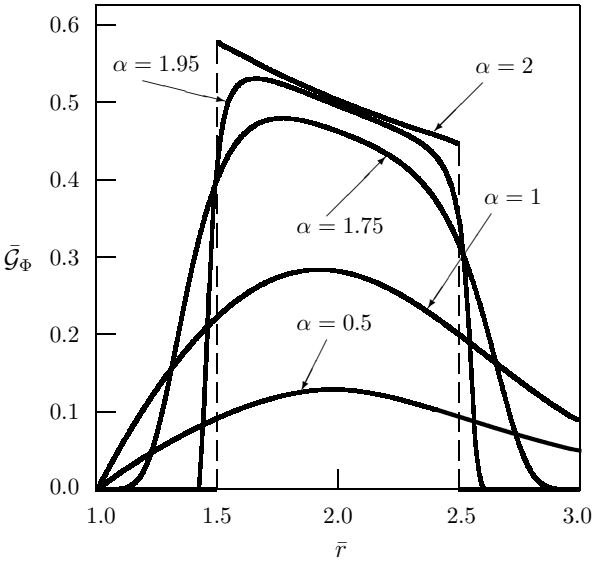

Figure 5.64: The fundamental solution to the source problem in a body with a cylindrical hole under zero Dirichlet boundary condition ($\bar{\rho} = 2$, $\kappa = 0.5$)

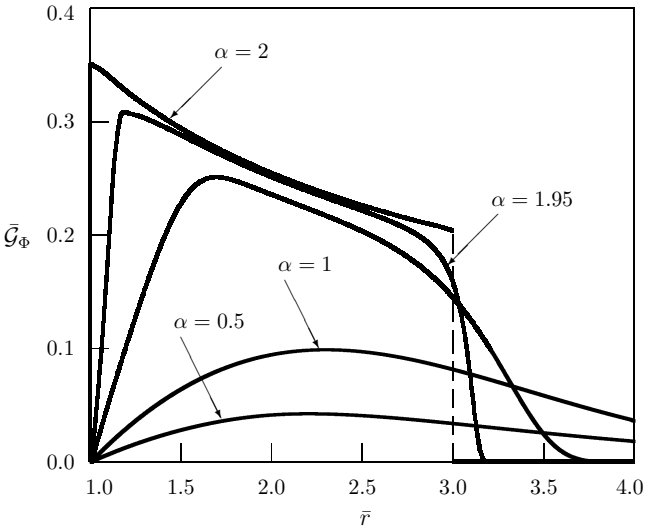

Figure 5.65: The fundamental solution to the source problem in a body with a cylindrical hole under zero Dirichlet boundary condition ($\bar{\rho} = 2$, $\kappa = 1$)

Fundamental solution to the Dirichlet problem

$$\frac{\partial^\alpha \mathcal{G}_g}{\partial t^\alpha} = a\left(\frac{\partial^2 \mathcal{G}_g}{\partial r^2} + \frac{1}{r}\frac{\partial \mathcal{G}_g}{\partial r}\right), \tag{5.129}$$

$$t = 0: \quad \mathcal{G}_g = 0, \qquad 0 < \alpha \le 2, \tag{5.130}$$

$$t = 0: \quad \frac{\partial \mathcal{G}_g}{\partial t} = 0, \qquad 1 < \alpha \le 2, \tag{5.131}$$

$$r = R: \quad \mathcal{G}_g = g_0\,\delta(t). \tag{5.132}$$

The solution [157]:

$$\mathcal{G}_g(r,t) = -\frac{2ag_0 t^{\alpha-1}}{\pi}\int_0^\infty E_{\alpha,\alpha}(-a\xi^2 t^\alpha) \times \frac{J_0(r\xi)Y_0(R\xi) - Y_0(r\xi)J_0(R\xi)}{J_0^2(R\xi) + Y_0^2(R\xi)}\,\xi\,\mathrm{d}\xi. \tag{5.133}$$

The fundamental solution $\overline{\mathcal{G}}_g = t\mathcal{G}_g/g_0$ is shown in Fig. 5.66. The plot of solution for $\alpha = 2$ in Fig. 5.66 needs additional discussion. If we consider the axisymmetric Cauchy problem for the wave equation in a plane with initial value $T(r,0) = \delta(r-R)$, then the nondimensional solution for $0 < \kappa < 1$ has the form

$$\overline{\mathcal{G}}_f = \frac{1}{2\sqrt{1-\kappa}}\,\delta(\bar{r} - 1 + \kappa) + \frac{1}{2\sqrt{1+\kappa}}\,\delta(\bar{r} - 1 - \kappa) + (\text{a “tail”}) \tag{5.134}$$

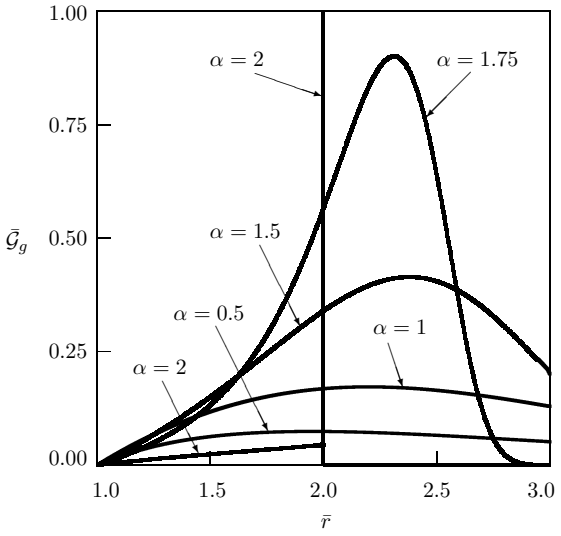

Figure 5.66: The fundamental solution to the Dirichlet problem for a body with a cylindrical hole ($\bar{\rho} = 2$, $\kappa = 1$) [157]

(see (5.16)). The first term in Eq. (5.134) presents the delta peak traveling in the direction of origin, the second term corresponds to the delta peak propagating in the direction of infinity, and the third term describes a "tail" behind the wave fronts. In the case of a cylinder with radius R ($0 \le r \le R$) the signaling problem for the wave equation with the Dirac delta boundary condition $T(R,t) = \delta(t)$ in the case $0 < \kappa < 1$ has a solution containing the delta peak traveling in the direction of origin and a portion of "tail" behind the wave front:

$$\overline{\mathcal{G}}_g = \frac{1}{\sqrt{1-\kappa}}\,\delta(\bar{r} - 1 + \kappa) \;+\; (\text{a "tail"}). \tag{5.135}$$

Similarly, in the case of an infinite medium with cylindrical cavity ($R \le r < \infty$) the corresponding solution to the signaling problem contains the delta peak traveling in the direction of infinity and also a portion of "tail" behind the wave front:

$$\overline{\mathcal{G}}_g = \frac{1}{\sqrt{1+\kappa}}\,\delta(\bar{r} - 1 - \kappa) \;+\; (\text{a "tail"}). \tag{5.136}$$

It should be noted that coefficients of delta functions in (5.135) and (5.136) are twice as large as those in (5.134) (the initial delta pulse does not split in two parts). The "tails" in (5.135) and (5.136) cannot be calculated analytically as in (5.134), but can be estimated numerically.

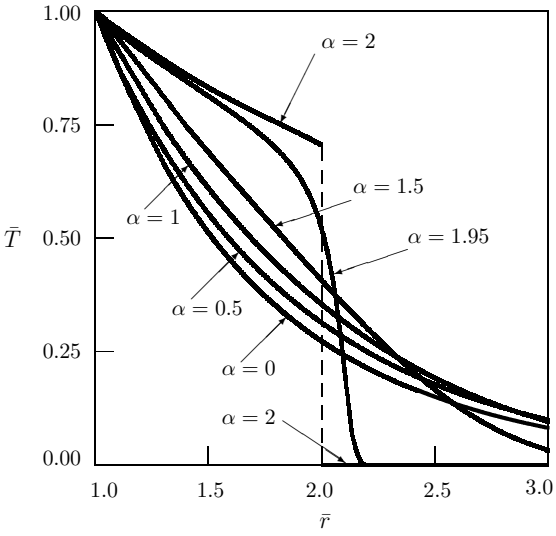

Figure 5.67: Dependence of the solution on distance (the Dirichlet problem for an infinite medium with cylindrical hole with constant boundary condition; $\kappa = 1$) [157]

Constant boundary value of temperature. In this case equations (5.129)–(5.131) are considered under the boundary condition

$$r = R: \quad T = T_0. \tag{5.137}$$

The solution has the following form [157]

$$T = T_0 + \frac{2T_0}{\pi} \int\limits_0^\infty E_\alpha(-a\xi^2 t^\alpha)\, \frac{J_0(r\xi)Y_0(R\xi) - Y_0(r\xi)J_0(R\xi)}{J_0^2(R\xi) + Y_0^2(R\xi)}\, \frac{\mathrm{d}\xi}{\xi} \tag{5.138}$$

and is displayed in Fig. 5.67 with $\overline{T} = T/T_0$.

Recall that the solution to the corresponding problem for the classical heat conduction equation is well known [26, 48]:

$$T = T_0 + \frac{2T_0}{\pi} \int\limits_0^\infty \exp\left(-a\xi^2 t\right)\, \frac{J_0(r\xi)Y_0(R\xi) - Y_0(r\xi)J_0(R\xi)}{J_0^2(R\xi) + Y_0^2(R\xi)}\, \frac{\mathrm{d}\xi}{\xi}. \tag{5.139}$$

5.4.2 Neumann boundary condition

$$\frac{\partial^\alpha T}{\partial t^\alpha} = a\left(\frac{\partial^2 T}{\partial r^2} + \frac{1}{r}\,\frac{\partial T}{\partial r}\right) + \Phi(r,t), \tag{5.140}$$

$$t = 0: \quad T = f(r), \qquad 0 < \alpha \le 2, \tag{5.141}$$

$$t = 0: \quad \frac{\partial T}{\partial t} = F(r), \quad 1 < \alpha \le 2, \tag{5.142}$$

$$r = R: \quad -\frac{\partial T}{\partial r} = g(t), \tag{5.143}$$

$$\lim_{r\to\infty} T(r,t) = 0. \tag{5.144}$$

The solution:

$$T(r,t) = \int_R^\infty f(\rho)\,\mathcal{G}_f(r,\rho,t)\,\rho\,\mathrm{d}\rho + \int_R^\infty F(\rho)\,\mathcal{G}_F(r,\rho,t)\,\rho\,\mathrm{d}\rho$$
$$+ \int_0^t \int_R^\infty \Phi(\rho,\tau)\,\mathcal{G}_\Phi(r,\rho,t-\tau)\,\rho\,\mathrm{d}\rho\,\mathrm{d}\tau + \int_0^t g(\tau)\,\mathcal{G}_g(r,t-\tau)\,\mathrm{d}\tau. \tag{5.145}$$

The fundamental solutions under zero Neumann boundary condition have the following form:

$$\begin{pmatrix} \mathcal{G}_f(r,\rho,t) \\ \mathcal{G}_F(r,\rho,t) \\ \mathcal{G}_\Phi(r,\rho,t) \end{pmatrix} = \int_0^\infty \begin{pmatrix} p_0\,E_\alpha(-a\xi^2 t^\alpha) \\ w_0 t\,E_{\alpha,2}(-a\xi^2 t^\alpha) \\ q_0 t^{\alpha-1}\,E_{\alpha,\alpha}(-a\xi^2 t^\alpha) \end{pmatrix} \frac{J_0(r\xi)\,Y_1(R\xi) - Y_0(r\xi)\,J_1(R\xi)}{J_1^2(R\xi) + Y_1^2(R\xi)}$$
$$\times \Big[J_0(\rho\xi)\,Y_1(R\xi) - Y_0(\rho\xi)\,J_1(R\xi)\Big]\,\xi\,\mathrm{d}\xi \tag{5.146}$$

and are obtained using the Laplace transform with respect to time t and the Weber transform (2.108), (2.119) with respect to the radial coordinate r.

Dependence of the fundamental solution $\bar{\mathcal{G}}_f = R^2\mathcal{G}_f/p_0$ on nondimensional distance $\bar{r} = r/R$ with $\bar{\rho} = \rho/R$ and $\kappa = \sqrt{a}t^\alpha/R$ is shown in Figs. 5.68 and 5.69. The fundamental solution $\bar{\mathcal{G}}_F = R^2\mathcal{G}_F/(w_0 t)$ is presented in Figs. 5.70 and 5.71. The fundamental solution to the source problem under zero Neumann boundary condition $\bar{\mathcal{G}}_\Phi = R^2\mathcal{G}_\Phi/(q_0 t^{\alpha-1})$ is depicted in Figs. 5.72 and 5.73. For $\kappa = 0.5$ the fundamental solutions under zero Dirichlet and Neumann boundary conditions are very similar (do not "feel" the boundary condition), but for $\kappa \ge 1$ the solutions under Dirichlet and Neumann boundary conditions are significantly different.

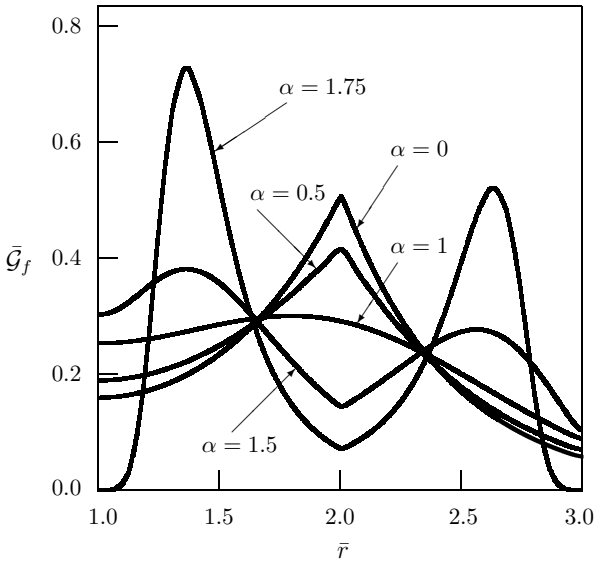

Figure 5.68: The fundamental solution to the first Cauchy problem in a body with a cylindrical hole under zero Neumann boundary condition ($\bar{\rho} = 2$, $\kappa = 0.5$)

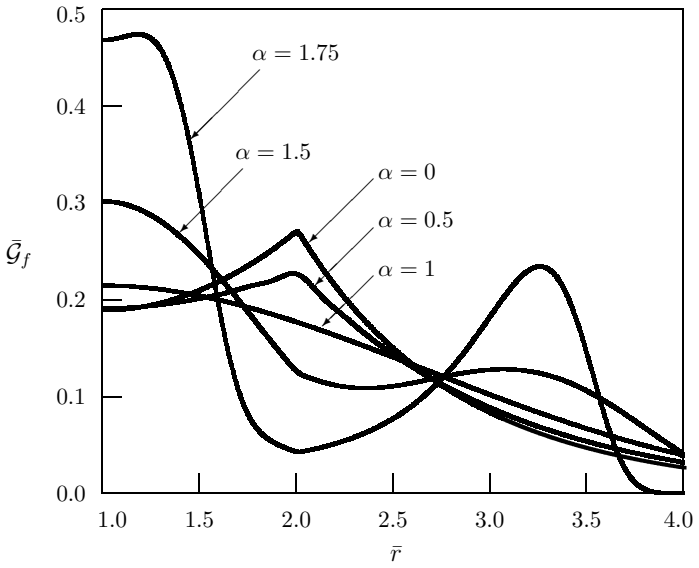

Figure 5.69: The fundamental solution to the first Cauchy problem in a body with a cylindrical hole under zero Neumann boundary condition ($\bar{\rho} = 2$, $\kappa = 1$)

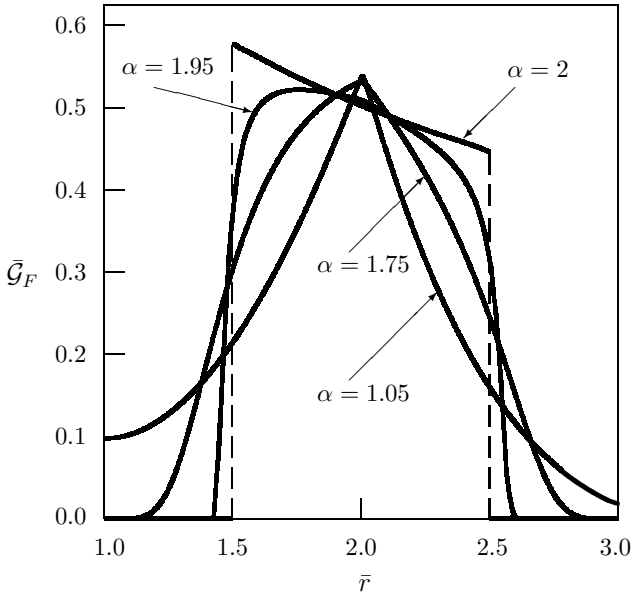

Figure 5.70: The fundamental solution to the second Cauchy problem in a body with a cylindrical hole under zero Neumann boundary condition ($\bar{\rho} = 2$, $\kappa = 0.5$)

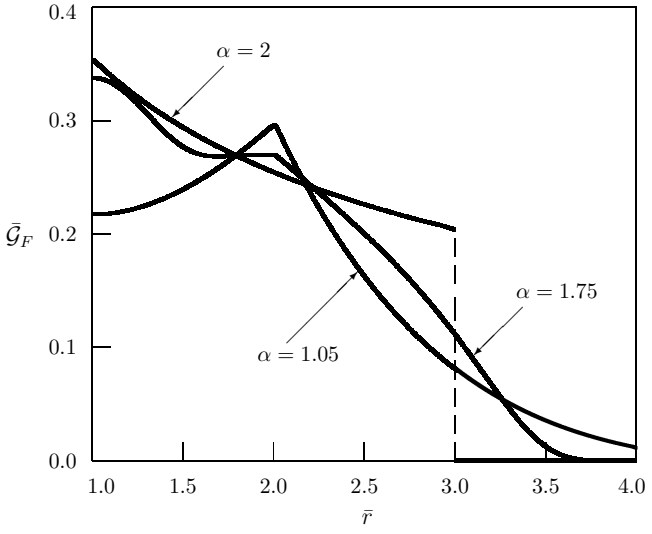

Figure 5.71: The fundamental solution to the second Cauchy problem in a body with a cylindrical hole under zero Neumann boundary condition ($\bar{\rho} = 2$, $\kappa = 1$)

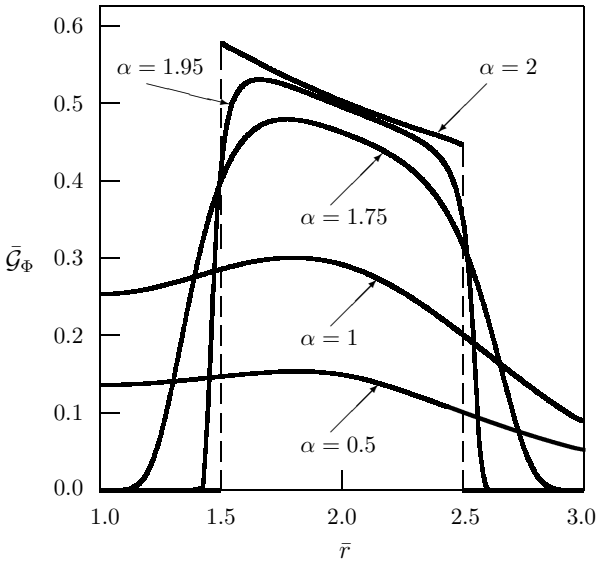

Figure 5.72: The fundamental solution to the source problem in a body with a cylindrical hole under zero Neumann boundary condition ($\bar{\rho} = 2$, $\kappa = 0.5$)

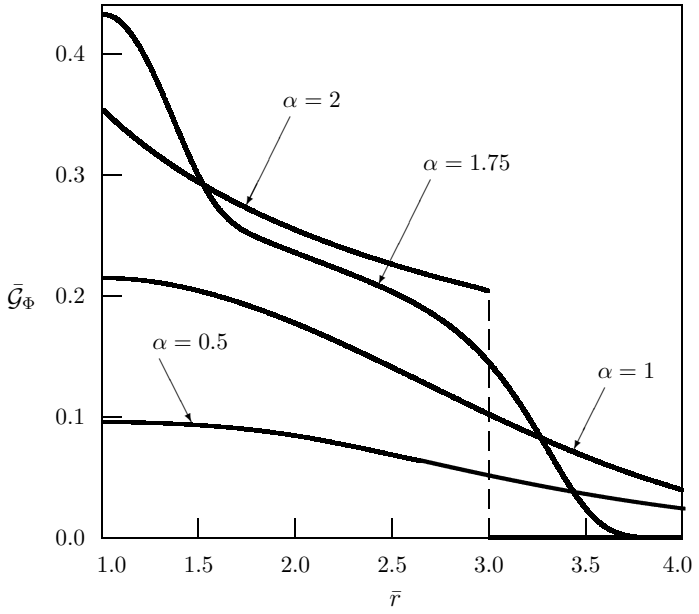

Figure 5.73: The fundamental solution to the source problem in a body with a cylindrical hole under zero Neumann boundary condition ($\bar{\rho} = 2$, $\kappa = 1$)

Fundamental solution to the mathematical Neumann problem

$$\frac{\partial^\alpha \mathcal{G}_m}{\partial t^\alpha} = a\left(\frac{\partial^2 \mathcal{G}_m}{\partial r^2} + \frac{1}{r}\,\frac{\partial \mathcal{G}_m}{\partial r}\right), \tag{5.147}$$

$$t = 0: \quad \mathcal{G}_m = 0, \qquad 0 < \alpha \le 2, \tag{5.148}$$

$$t = 0: \quad \frac{\partial \mathcal{G}_m}{\partial t} = 0, \qquad 1 < \alpha \le 2, \tag{5.149}$$

$$r = R: \quad \frac{\partial \mathcal{G}_m}{\partial r} = -g_0\,\delta(t). \tag{5.150}$$

The solution

$$\mathcal{G}_m(r,t) = -\frac{2ag_0 t^{\alpha-1}}{\pi}\int\limits_0^\infty E_{\alpha,\alpha}(-a\xi^2 t^\alpha)\,\frac{J_0(r\xi)Y_1(R\xi) - Y_0(r\xi)J_1(R\xi)}{J_1^2(R\xi) + Y_1^2(R\xi)}\,\mathrm{d}\xi. \tag{5.151}$$

is depicted in Fig. 5.74 with $\overline{\mathcal{G}}_m = t\mathcal{G}_m/(Rg_0)$.

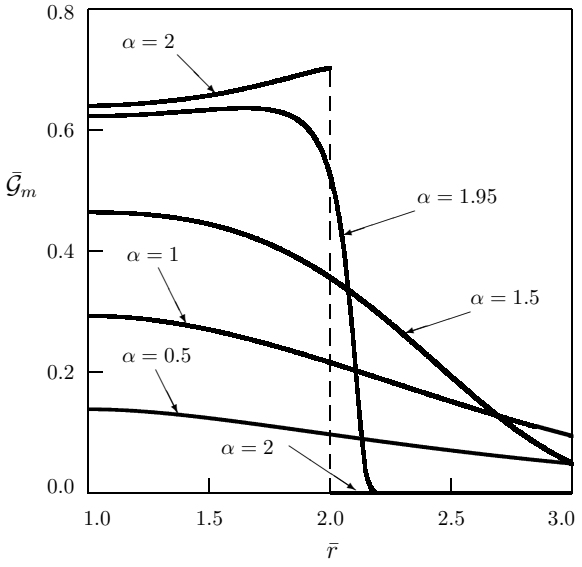

Figure 5.74: The fundamental solution to the mathematical Neumann problem for a body with a cylindrical hole ($\bar{\rho} = 2$, $\kappa = 1$) [157]

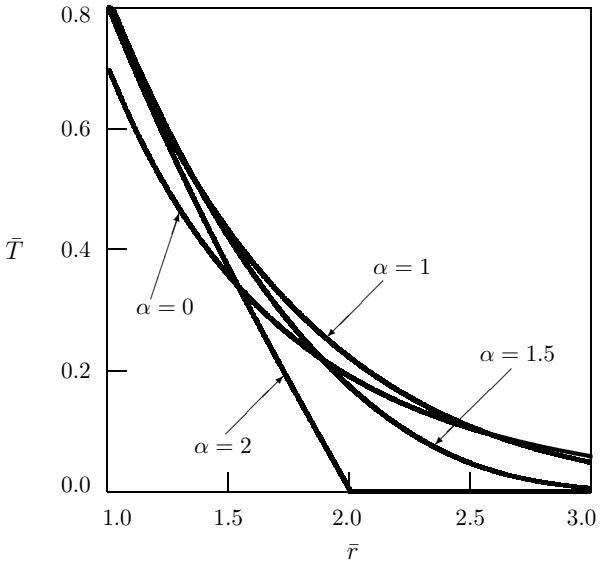

Figure 5.75: Dependence of the solution on distance (an infinite medium with a cylindrical hole and constant boundary value of normal derivative; $\kappa = 1$) [175]

Constant boundary value of normal derivative

$$r = R: \quad \frac{\partial T}{\partial r} = -g_0 = \text{const.} \tag{5.152}$$

The solution [157]

$$T = -\frac{2g_0}{\pi} \int_0^\infty \left[1 - E_\alpha(-a\xi^2 t^\alpha)\right] \frac{J_0(r\xi)Y_1(R\xi) - Y_0(r\xi)J_1(R\xi)}{J_1^2(R\xi) + Y_1^2(R\xi)} \frac{\mathrm{d}\xi}{\xi^2} \tag{5.153}$$

is shown in Fig. 5.75 ($\overline{T} = T/(Rg_0)$).

Fundamental solution to the physical Neumann problem

$$\frac{\partial^\alpha \mathcal{G}_p}{\partial t^\alpha} = a\left(\frac{\partial^2 \mathcal{G}_p}{\partial r^2} + \frac{1}{r}\frac{\partial \mathcal{G}_p}{\partial r}\right), \tag{5.154}$$

$$t = 0: \quad \mathcal{G}_p = 0, \qquad 0 < \alpha \le 2, \tag{5.155}$$

$$t = 0: \quad \frac{\partial \mathcal{G}_p}{\partial t} = 0, \qquad 1 < \alpha \le 2, \tag{5.156}$$

$$r = R: \quad D_{RL}^{1-\alpha}\frac{\partial \mathcal{G}_p}{\partial r} = -g_0\,\delta(t), \quad 0 < \alpha \le 1, \tag{5.157}$$

$$r = R: \quad I^{\alpha-1}\frac{\partial}{\partial r}\mathcal{G}_p = -g_0\,\delta(t), \quad 1 < \alpha \le 2. \tag{5.158}$$

The solution

$$\mathcal{G}_p(r,t) = -\frac{2ag_0}{\pi}\int\limits_0^\infty E_\alpha(-a\xi^2 t^\alpha)\,\frac{J_0(r\xi)Y_1(R\xi) - Y_0(r\xi)J_1(R\xi)}{J_1^2(R\xi) + Y_1^2(R\xi)}\,\mathrm{d}\xi. \tag{5.159}$$

Constant boundary value of the heat flux

$$r = R: \quad D_{RL}^{1-\alpha}\frac{\partial T}{\partial r} = -g_0, \qquad 0 < \alpha \le 1, \tag{5.160}$$

$$r = R: \quad I^{\alpha-1}\frac{\partial T}{\partial r} = -g_0, \qquad 1 < \alpha \le 2\,. \tag{5.161}$$

The solution

$$T = -\frac{2ag_0 t}{\pi}\int\limits_0^\infty E_{\alpha,2}(-a\xi^2 t^\alpha)\,\frac{J_0(r\xi)Y_1(R\xi) - Y_0(r\xi)J_1(R\xi)}{J_1^2(R\xi) + Y_1^2(R\xi)}\,\mathrm{d}\xi \tag{5.162}$$

is shown in Fig. 5.76 with $\overline{T} = RT/(ag_0 t)$.

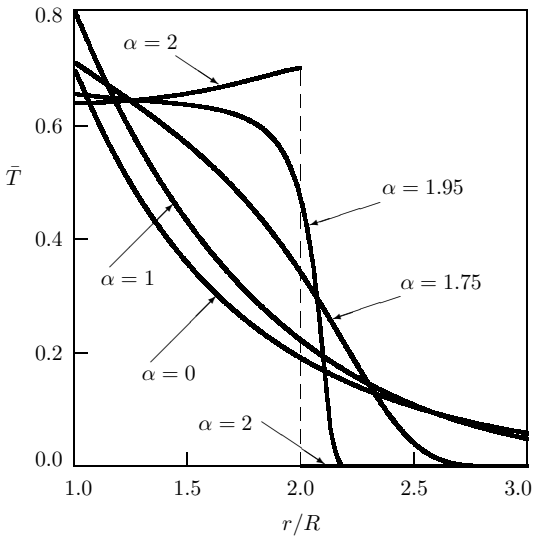

Figure 5.76: Dependence of the temperature on distance (the constant heat flux at the boundary of a body with a cylindrical hole) [175]

5.4.3 Robin boundary condition

$$\frac{\partial^\alpha T}{\partial t^\alpha} = a\left(\frac{\partial^2 T}{\partial r^2} + \frac{1}{r}\,\frac{\partial T}{\partial r}\right) + \Phi(r,t), \tag{5.163}$$

$$t = 0: \quad T = f(r), \qquad 0 < \alpha \le 2, \tag{5.164}$$

$$t = 0: \quad \frac{\partial T}{\partial t} = F(r), \quad 1 < \alpha \le 2, \tag{5.165}$$

$$r = R: \quad -\frac{\partial T}{\partial r} + HT = g(t), \tag{5.166}$$

$$\lim_{r\to\infty} T(r,t) = 0. \tag{5.167}$$

The solution:

$$T(r,t) = \int\limits_R^\infty f(\rho)\,\mathcal{G}_f(r,\rho,t)\,\rho\,\mathrm{d}\rho + \int\limits_R^\infty F(\rho)\,\mathcal{G}_F(r,\rho,t)\,\rho\,\mathrm{d}\rho$$

$$+ \int\limits_0^t \int\limits_R^\infty \Phi(\rho,\tau)\,\mathcal{G}_\Phi(r,\rho,t-\tau)\,\rho\,\mathrm{d}\rho\,\mathrm{d}\tau + \int\limits_0^t g(\tau)\,\mathcal{G}_g(r,t-\tau)\,\mathrm{d}\tau. \tag{5.168}$$

The fundamental solutions under zero Robin boundary condition

$$\begin{pmatrix} \mathcal{G}_f(r,\rho,t) \\ \mathcal{G}_F(r,\rho,t) \\ \mathcal{G}_\Phi(r,\rho,t) \end{pmatrix} = \int\limits_0^\infty \begin{pmatrix} p_0\,E_\alpha(-a\xi^2 t^\alpha) \\ w_0 t\,E_{\alpha,2}(-a\xi^2 t^\alpha) \\ q_0 t^{\alpha-1}\,E_{\alpha,\alpha}(-a\xi^2 t^\alpha) \end{pmatrix}$$

$$\times \frac{Y_0(r\xi)\,[\xi J_1(R\xi) + HJ_0(R\xi)] - J_0(r\xi)\,[\xi Y_1(R\xi) + HY_0(R\xi)]}{[\xi J_1(R\xi) + HJ_0(R\xi)]^2 + [\xi Y_1(R\xi) + HY_0(R\xi)]^2}$$

$$\times \big\{ Y_0(\rho\xi)\,[\xi J_1(R\xi) + HJ_0(R\xi)] - J_0(\rho\xi)\,[\xi Y_1(R\xi) + HY_0(R\xi)] \big\}\,\xi\mathrm{d}\xi \tag{5.169}$$

are obtained using the Laplace transform with respect to time t and the Weber transform (2.108), (2.121) with respect to the radial coordinate r.

The fundamental solution to the mathematical Robin problem under zero initial conditions has the following form:

$$\mathcal{G}_g(r,t) = \frac{2ag_0 t^{\alpha-1}}{\pi} \int\limits_0^\infty E_{\alpha,\alpha}(-a\xi^2 t^\alpha)$$

$$\times \frac{Y_0(r\xi)\,[\xi J_1(R\xi) + HJ_0(R\xi)] - J_0(r\xi)\,[\xi Y_1(R\xi) + HY_0(R\xi)]}{[\xi J_1(R\xi) + HJ_0(R\xi)]^2 + [\xi Y_1(R\xi) + HY_0(R\xi)]^2}\,\xi\mathrm{d}\xi. \tag{5.170}$$